Closed-form solutions to the dynamics of confined biased lattice random walks in arbitrary dimensions

Seeralan Sarvaharman[1,*] and Luca Giuggioli [1,2,†]

[1]*Department of Engineering Mathematics, University of Bristol, BS8 1UB, United Kingdom*
[2]*Bristol Centre for Complexity Sciences, University of Bristol, BS8 1UB, United Kingdom*

Biased lattice random walks (BLRW) are used to model random motion with drift in a variety of empirical situations in engineering and natural systems such as phototaxis, chemotaxis, or gravitaxis. When motion is also affected by the presence of external borders resulting from natural barriers or experimental apparatuses, modelling biased random movement in confinement becomes necessary. To study these scenarios, confined BLRW models have been employed but so far only through computational techniques due to the lack of an analytic framework. Here, we lay the groundwork for such an analytical approach by deriving the Green's functions, or propagators, for the confined BLRW in arbitrary dimensions and arbitrary boundary conditions. By using these propagators we construct explicitly the time-dependent first-passage probability in one dimension for reflecting and periodic domains, while in higher dimensions we are able to find its generating function. The latter is used to find the mean first-passage passage time for a d-dimensional box, d-dimensional torus or a combination of both. We show the appearance of surprising characteristics such as the presence of saddles in the spatiotemporal dynamics of the propagator with reflecting boundaries, bimodal features in the first-passage probability in periodic domains and the minimization of the mean first-return time for a bias of intermediate strength in rectangular domains. Furthermore, we quantify how in a multitarget environment with the presence of a bias shorter mean first-passage times can be achieved by placing fewer targets close to boundaries in contrast to many targets away from them.

I. INTRODUCTION

Random walk models have been ubiquitously applied across a variety of disciplines both with continuous space-time variables, i.e., Brownian walks [1], and with discrete variables (in space and time), i.e., lattice random walks (LRW) [2]. Due to their simplicity, LRW have been used as null models to understand the stochastic dynamics in polymer chains [3], record statistics [4], population genetics [5], foraging behavior in animals [6], diffusion on the surface of stars [7], energy transfer in molecules [8,9], and protein transport along DNA [10,11], to name just a few. LRW have also inspired many theoretical approaches to study coverage times [12,13], resetting random walks [14], and anomalous dynamics in disordered systems [15].

For many real systems, the use of LRW has provided a convenient way to extract information about the statistics of an important quantity, the so-called first-passage probability, or a related one, the so-called first-return probability. They measure the probability that a random variable has reached or returned to a given value for the first time. These quantities represent a work-horse in random search processes and, more generally, in transport calculations [16–18]. In many empirical scenarios, when natural or artificial barriers resulting from

experimental apparatuses affect the dynamics, LRW models need to be modified to account for the presence of boundaries. The effects on the first passage statistics become quite significant when the spatial domain is bounded as exemplified by the mean return time (MRT) and mean first-passage time (MFPT) becoming finite as compared to infinite when space is unbounded. Explicit expressions for the MRT have been established long ago [19], those for the MFPT up to 3D for both rectangular and periodic lattices have been known for some time [20,21], while the analogous ones in higher-dimensional cases have been found more recently [22].

Despite the large amount of analytic studies on LRW in confined space and their related first-passage statistics [18,23,24], there has been no attempt to generalise the expressions for the MRT or the MFPT when motion is not completely random but possesses a bias in some direction, the so-called biased lattice random walks (BLRW). Similarly there has been no analytic progress for the first-passage and return probability, with studies on confined BLRW having been mainly computational [25–28]. This is somewhat surprising given that there are significant areas of research where BLRW models are employed. They include biological systems such as cell migration due to concentration gradients (chemotaxis) [25,26], bacteria drifting toward a light source (phototaxis) [27], or upwards movement of single-celled algae in response to gravity (gravitaxis) [29]. In engineering it is worth mentioning the application of BLRW to study routing protocol for wireless sensor networks [30], to analyze the

---

*s.sarvaharman@bristol.ac.uk

†Luca.Giuggioli@bristol.ac.uk

degradation of pavement [28] and to model field-driven translocation of tracer particles [31].

With the only closed-form results for BLRW in finite domains pertaining to the generating function of the 1D propagator with two absorbing boundaries [32], there is a need to develop a general framework that allows to derive analytically various transport quantities. Here we are able to do so by extending the LRW techniques in Ref. [22] to construct analytically the confined time-dependent propagator and its generating function for BLRW in arbitrary dimensions and arbitrary boundary conditions. These propagators are then used to study first-passage and first-return statistics and obtain analytic expressions for the MRT and MFPT.

The remainder of the paper is organized as follows. Section II deals with BLRW in 1D; it develops a symmetrization procedure that allows to impose different boundary conditions and find the propagator generating functions. The time-dependent propagators are also presented. The derivation of time-dependent first-passage probabilities and mean first-passage times using the propagator expressions form Sec. III. In Sec. IV we treat the problem in higher dimensions, using a hierarchical procedure to obtain BLRW propagators in arbitrary dimensions and arbitrary boundary conditions. Using these results we derive the MFPT in d-dimension with reflecting boundaries (d-box), periodic boundaries (d-torus), or a mixture of periodic and reflecting boundaries. Last, a summary of the findings are presented in Sec. V.

II. TIME-DEPENDENT PROPAGATORS IN ONE DIMENSION

We start by considering the dynamics of a random walker with bias on a 1D infinite lattice. It is conveniently described by utilizing two parameters q and g. The parameter q controls the "diffusivity," with $q = 0$ representing a walker that never moves, while $q = 1$ a walker that moves at each time step. We take the probability of jumping to the neighboring site on the left as $\frac{q}{2}(1 + g)$, while the probability of jumping to the right as $\frac{q}{2}(1 - g)$, and $1 - q$ as the probability of not moving. The parameter g controls the strength of the bias. When $g = 0$, the movement is diffusive, whereas the cases $g = 1$ and $g = -1$ are, respectively, the ballistic limit to the left and right. The dynamics are governed by the Master equation

$$P(n, t + 1) = (1 - q)P(n, t) + \frac{q}{2}(1 - g)P(n - 1, t)$$
$$+ \frac{q}{2}(1 + g)P(n + 1, t), \quad (1)$$

with n representing the lattice site and t the discrete time variable. The solution of Eq. (1) can be obtained by Fourier transforming, $\widehat{P}(\kappa, t) = \sum_{n=-\infty}^{\infty} P(n, t)e^{-i\kappa n}$, subsequently by finding the generating function and finally by inverse transforming to real space to obtain [32]

$$\widetilde{P}_{n_0}(n, z) = \frac{\eta f^{\frac{n - n_0}{2}} \alpha^{-|n - n_0|}}{zq \sinh\left[\operatorname{acosh}\left(\frac{\eta}{\beta}\right)\right]}, \quad (2)$$

with $\widetilde{P}(n, z) = \sum_{t=0}^{\infty} P(n, t)z^t$ and with n_0 indicating the localized initial condition $P(n, 0) = \delta_{n,n_0}$, where δ is a Kronecker delta. For convenience we have employed the

following notation:

$$f = \frac{1 - g}{1 + g}, \quad \eta = \frac{1 + f}{2\sqrt{f}}, \quad \beta = \frac{zq}{1 - z(1 - q)},$$
$$\alpha = \exp\left[\operatorname{acosh}\left(\frac{\eta}{\beta}\right)\right], \quad (3)$$

and the subscript notation P_{n_0} to denote a localized initial condition at $n = n_0$. The absence of a bias, that is $g \to 0$, implies that $f, \eta \to 1$, and one recovers the expression of the propagator of the so-called lazy lattice walker [22], that is a Polya's walk where the walker may also stay put at each time step.

A. Symmetrization procedure in presence of boundaries

When imposing boundary conditions, the method of images is an intuitive and effective technique to solve the Master equation. However, when the dynamics are spatially asymmetric, the method breaks down. If one wishes to employ it, the Master equation needs to be made symmetric first. This can be accomplished using a technique used originally by Montroll [33]. That technique was used to construct the propagator for a biased continuous-time random walk in presence of a single boundary. Here we extend that technique to multiple boundaries and discrete time. Applying the transformation

$$Q(n, t) = f^{-\frac{n}{2}} P(n, t)\omega^t - \mu f^{-\frac{n+1}{2}} P(n + 1, t)\omega^t \quad (4)$$

to Eq. (1), or applying its equivalent in z domain,

$$\widetilde{Q}(n, z) = f^{-\frac{n}{2}} \widetilde{P}(n, z\omega) - \mu f^{-\frac{n+1}{2}} \widetilde{P}(n + 1, z\omega), \quad (5)$$

where $\mu \geqslant 0$ and $\omega^{-1} = 1 - q + \frac{q}{\eta}$, results in a symmetrized dynamics given by

$$Q(n, t + 1) = \omega(1 - q)Q(n, t)$$
$$+ \frac{q\omega}{2\eta}[Q(n - 1, t) + Q(n + 1, t)]. \quad (6)$$

To transform back from the symmetric probability $\widetilde{Q}(n, z)$ to the original $\widetilde{P}(n, z)$, one exploits the recursive nature of transformation Eq. (5) to write

$$\widetilde{P}(n, z) = f^{\frac{n}{2}} \sum_{j=0}^{\infty} \mu^j \widetilde{Q}\left(m + j, \frac{z}{\omega}\right), \quad (7)$$

where $\widetilde{Q}(n, z)$ is the general solution to Eq. (6) in z domain. The corresponding initial condition of $Q(n, t)$ is related to that of $P(n, t)$ via $Q(n, 0) = f^{-\frac{n}{2}} P(n, 0) - \mu f^{-\frac{n+1}{2}} P(n, 0)$. The general solution of Eq. (6) is given by

$$\widetilde{Q}(n, z) = \sum_{m=-\infty}^{\infty} Q(m, 0)\widetilde{H}_m(n, z), \quad (8)$$

where [22]

$$\widetilde{H}_{n_0}(n, z) = \frac{\eta \varphi^{-|n - n_0|}}{z\omega q \sinh\left[\operatorname{acosh}\left(\frac{1}{\zeta}\right)\right]} \quad (9)$$

is the propagator of Eq. (6) and with

$$\zeta = \frac{z\omega q}{\eta[1 - z\omega(1 - q)]} \quad (10)$$
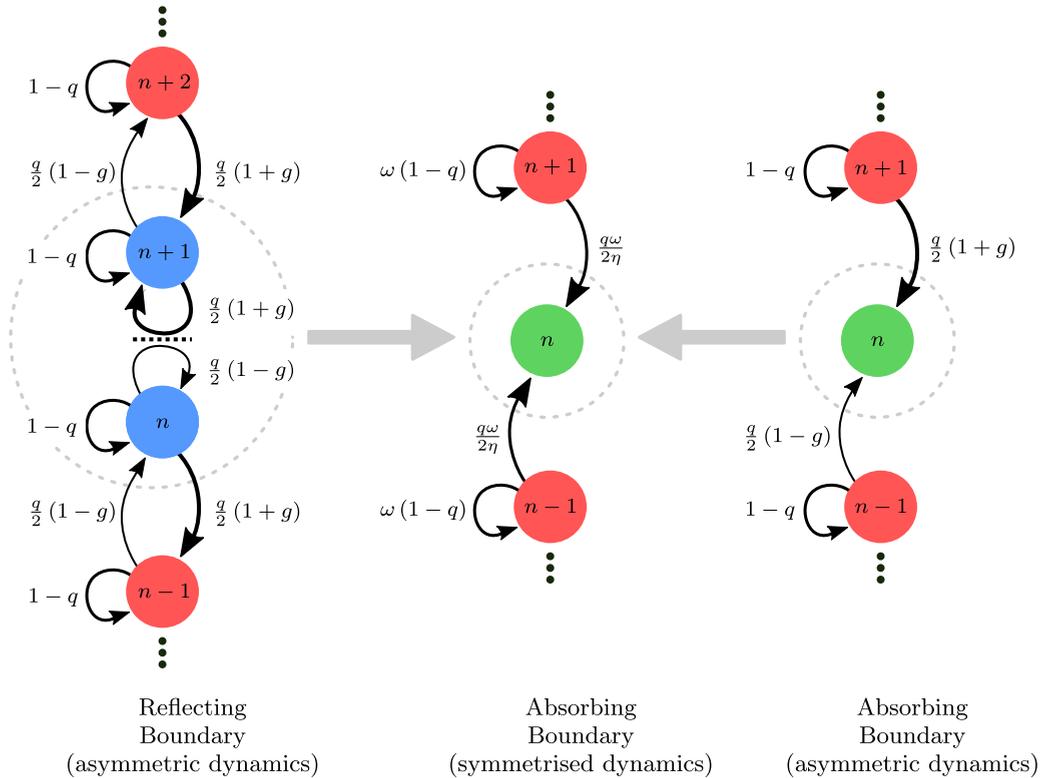
FIG. 1. Schematic diagram showing the effect of the symmetrizing transformation Eq. (4) or Eq. (5) on a single reflecting (leftmost) or a single absorbing (rightmost) boundary with the lattices displayed vertically. The red circles represent sites in the bulk of the domain, the blue circles represent sites adjacent to a reflecting boundary shown as a dashed black line and the green circles are absorbing sites. A reflecting boundary is a constraint imposed on two sites: With the barrier between the sites n and $n + 1$, the flux between them must be zero. In so doing the probability of not moving at these sites becomes $1 - \frac{q}{2}(1 - g)$ or $1 - \frac{q}{2}(1 + g)$ for the site above the boundary $n + 1$ or below the boundary n, respectively. An absorbing boundary is a constraint on a single lattice site where the probability at the site must be zero. Under the transformation, both the reflective boundary between sites n and $n + 1$ and the absorbing boundary at n with asymmetric dynamics become an absorbing site n with symmetric dynamics.

and

$$\varphi = \exp\left[\mathrm{acosh}\left(\frac{1}{\zeta}\right)\right]. \quad (11)$$

Using the symmetric solution Eq. (9), it becomes possible to apply the method of images for various types of boundary conditions. In the following sections, to distinguish the different cases, we use the calligraphic notation, i.e., $\mathcal{P}^{(\gamma)}$ and $\mathcal{Q}^{(\gamma)}$, for semibounded domains, and $P^{(\gamma)}$ and $Q^{(\gamma)}$ for finite domains where $\gamma = a, r, m, p$ represents, respectively, absorbing, reflecting, mixed (one reflecting and one absorbing) and periodic boundary conditions. The unbounded occupation probability is represented by P and Q without any superscript γ.

B. Semibounded propagators

For semi-infinite domains we consider bias random walks on $\mathbb{Z}^+$. The two straightforward types of boundary conditions that one can impose are a single reflection and a single absorption; they are pictorially represented in Fig. 1. In both of these cases, the semibounded propagator is constructed as a superposition of two unbounded propagators. For a single absorbing boundary at $n = 1$, the requirement $\widetilde{P}(1, z) = 0$ corresponds, in the symmetric propagator, to $\widetilde{Q}(1, z) = 0$

and with $\mu = 0$. The boundary condition is satisfied using a single mirror image giving the general solution $\widetilde{\mathcal{Q}}^{(a)}(n, z) = \sum_{m=1}^{\infty} \mathcal{Q}^{(a)}(m, 0)[\widetilde{H}_m(n, z) - \widetilde{H}_{2-m}(n, z)]$, where the spatial convolution is over the semi-infinite domain and where $\mathcal{Q}^{(a)}(m, 0)$ is the initial condition after symmetrization, that is obtained from Eq. (4) when $t = 0$. For an initial condition $\mathcal{P}^{(a)}(n, 0) = \delta_{n,n_0}$ the propagator with a single absorbing boundary at site $n = 1$ is

$$\widetilde{\mathcal{P}}^{(a)}_{n_0}(n, z) = \frac{\eta f^{\frac{n - n_0}{2}}(\alpha^{-|n - n_0|} - \alpha^{-|n + n_0 - 2|})}{zq \sinh\left[\mathrm{acosh}\left(\frac{\eta}{\beta}\right)\right]}. \quad (12)$$

A reflective boundary condition on the asymmetric propagator requires the flux across the boundary to be zero. With the boundary between site $n = 0$ and $n = 1$, the zero flux condition is given by $f\widetilde{P}(0, z) - \widetilde{P}(1, z) = 0$. The corresponding conditions on the symmetric propagator are $\mu = f^{-\frac{1}{2}}$ and $\widetilde{Q}(0, z) = 0$. With $\mu \neq 0$, under the transformation Eq. (5), the space between the lattice in the P domain become sites in the Q domain and vice versa. The zero flux boundary condition is transformed into an absorbing one that is satisfied using a single image and a symmetrized initial condition $\mathcal{Q}^{(a)}(n, 0)$, i.e., $\widetilde{\mathcal{Q}}^{(a)}(n, z) = \sum_{m=0}^{\infty} \mathcal{Q}^{(a)}(m, 0)[\widetilde{H}_m(n, z) - \widetilde{H}_{-m}(n, z)]$, where once again $\mathcal{Q}^{(a)}(m, 0)$ is the initial condition obtained from Eq. (4) when

$t = 0$. Transforming back to the original propagator using Eq. (7) is quite involved and key steps are given in Appendix A 1. For an initial condition $\mathcal{P}^{(r)}(n, 0) = \delta_{n,n_0}$ the propagator with a single reflective boundary between sites $n = 0$ and $n = 1$ is given by

$$\widetilde{\mathcal{P}}_{n_0}^{(r)}(n, z) = \frac{\eta f^{\frac{n-n_0}{2}}(\alpha^{-|n-n_0|} - \alpha^{-|n+n_0|}\xi)}{zq \sinh\left[\text{acosh}\left(\frac{\eta}{\beta}\right)\right]}, \qquad (13)$$

where

$$\xi = \frac{f^{\frac{1}{2}} - \alpha}{f^{\frac{1}{2}} - \alpha^{-1}}. \qquad (14)$$

In Fig. 1 we display pictorially the two transformations in the absorbing and reflecting cases, both leading to an absorbing boundary condition in the symmetrized case.

C. Bounded propagators

Having studied propagators on a semi-infinite domain we now turn to random walks on the finite 1D lattice $1 \leqslant n \leqslant N$. We start with the simplest of these cases, a finite domain with two absorbing walls. In addition to the absorbing site $n = 1$ we have an absorbing boundary at $n = N$ giving the further constraint $\widetilde{P}(N, z) = 0$, which corresponds to the condition $\widetilde{Q}(N, z) = 0$ and $\mu = 0$ in Eq. (5). In this case, the bounded solution is constructed with infinite images of the unbounded propagators and the convolution is only over sites within the domain, $\widetilde{Q}^{(a)}(n, z) = \sum_{m=1}^{N}\sum_{k=-\infty}^{+\infty} Q^{(a)}(m, 0)[\widetilde{H}_{m-2k(N-1)}(n, z) - \widetilde{H}_{2-m-2k(N-1)}(n, z)]$, where $Q^{(a)}(m, 0)$ is the symmetrized initial condition in a finite domain obtained from Eq. (D4). With a localized initial condition, $P^{(a)}(n, 0) = \delta_{n,n_0}$, after computing the double summation the propagator with two absorbing boundaries is

$$\widetilde{P}_{n_0}^{(a)}(n, z) = \frac{\eta f^{\frac{n-n_0}{2}}}{zq \sinh\left[\text{acosh}\left(\frac{\eta}{\beta}\right)\right]} \left\{ \frac{2 \sinh\left[(N - n_>)\text{acosh}\left(\frac{\eta}{\beta}\right)\right] \sinh\left[(n_< - 1)\text{acosh}\left(\frac{\eta}{\beta}\right)\right]}{\sinh\left[(N - 1)\text{acosh}\left(\frac{\eta}{\beta}\right)\right]} \right\}, \qquad (15)$$

where we use the notation $n_> = \frac{1}{2}(n + n_0 + |n - n_0|)$ and $n_< = \frac{1}{2}(n + n_0 - |n - n_0|)$.

For two reflective boundaries we consider a domain with two impenetrable barriers: The first between the sites $n = 0$ and $n = 1$, the second between the sites $n = N$ and $n = N + 1$, thus imposing the constraints $f\widetilde{P}(0, z) - \widetilde{P}(1, z) = 0$ and $f\widetilde{P}(N, z) - \widetilde{P}(N + 1, z) = 0$, respectively. With the choice $\mu = f^{-\frac{1}{2}}$ in Eq. (5), these constraints corresponds to the conditions $\widetilde{Q}(0, z) = 0$ and $\widetilde{Q}(N, z)$ on the symmetric propagator We follow the same procedure as the absorbing case by constructing the bounded solution with infinite images of the unbounded propagator, $\widetilde{Q}^{(a)}(n, z) = \sum_{m=0}^{N}\sum_{k=-\infty}^{+\infty} Q^{(a)}(m, 0)[\widetilde{H}_{m+2kN}(n, z) - \widetilde{H}_{-m+2kN}(n, z)]$, where once again $Q^{(a)}(m, 0)$ is the initial condition after symmetrization from Eq. (4) (for a full derivation see Appendix A 2). With the initial condition $P^{(r)}(n, 0) = \delta_{n,n_0}$, the resulting propagator with two reflective boundaries is

$$\widetilde{P}_{n_0}^{(r)}(n, z) = \frac{f^{\frac{n-n_0-1}{2}}\left\{f^{\frac{1}{2}}\sinh\left[(N - n_>)\text{acosh}\left(\frac{\eta}{\beta}\right)\right] - \sinh\left[(N + 1 - n_>)\text{acosh}\left(\frac{\eta}{\beta}\right)\right]\right\}}{(z - 1)\sinh\left[\text{acosh}\left(\frac{\eta}{\beta}\right)\right]\sinh\left[N\text{acosh}\left(\frac{\eta}{\beta}\right)\right]}$$

$$\times \left\{f^{\frac{1}{2}}\sinh\left[n_<\text{acosh}\left(\frac{\eta}{\beta}\right)\right] - \sinh\left[(n_< - 1)\text{acosh}\left(\frac{\eta}{\beta}\right)\right]\right\}. \qquad (16)$$

For the mixed boundary condition (reflecting between $n = 0$ and $n = 1$ and absorbing at $n = N$) we take the propagator with a single reflective boundary given in Eq. (13), and construct the propagator by considering the probability of being at site n and having not visited the boundary site N [34], $P_{n_0}^{(m)}(n, t) = \mathcal{P}_{n_0}^{(r)}(n, t) - \sum_{t'=0}^{t} F_{n_0}^{(r)}(N, t')\mathcal{P}_N^{(r)}(n, t - t')$, where $F_{n_0}^{(r)}(n, t)$ is the first-passage probability of being at site n at time t for a walker that started at site n_0 in a lattice with an impenetrable barrier between $n = 0$ and $n = 1$. In z-domain the relation is simply $\widetilde{P}_{n_0}^{(m)}(n, z) = \widetilde{\mathcal{P}}_{n_0}^{(r)}(n, z) - \widetilde{F}_{n_0}^{(r)}(N, z)\widetilde{\mathcal{P}}_N^{(r)}(n, z)$ where $\widetilde{F}_{n_0}^{(r)}(N, z)$ can be found in Eq. (D1). After some algebra one finds the expression

$$\widetilde{P}_{n_0}^{(m)}(n, z) = \frac{2f^{\frac{n-n_0}{2}}\eta \sinh\left[(N - n_>)\text{acosh}\left(\frac{\eta}{\beta}\right)\right]\left\{f^{\frac{1}{2}}\sinh\left[n_<\text{acosh}\left(\frac{\eta}{\beta}\right)\right] - \sinh\left[(n_< - 1)\text{acosh}\left(\frac{\eta}{\beta}\right)\right]\right\}}{zq \sinh\left[\text{acosh}\left(\frac{\eta}{\beta}\right)\right]\left\{f^{\frac{1}{2}}\sinh\left[N\text{acosh}\left(\frac{\eta}{\beta}\right)\right] - \sinh\left[(N - 1)\text{acosh}\left(\frac{\eta}{\beta}\right)\right]\right\}}. \qquad (17)$$

Last, we consider a biased random walk on a 1D periodic domain with N distinct sites, which implies that $\widetilde{P}(n, z) = \widetilde{P}(n + kN, z)$ for any integer k. To satisfy the boundary condition one simply wraps the unbounded propagator Eq. (2) via the summation $\widetilde{P}_{n_0}^{(p)}(n, z) = \sum_{k=-\infty}^{\infty} \widetilde{P}_{n_0}(n + kN, z)$. Evaluating the sum yields

$$\widetilde{P}_{n_0}^{(p)}(n, z) = \frac{\eta f^{\frac{n-n_0}{2}}\left\{\sinh\left[(N - |n - n_0|)\text{acosh}\left(\frac{\eta}{\beta}\right)\right] + f^{-\frac{N\,\text{sgn}(n-n_0)}{2}}\sinh\left[|n - n_0|\text{acosh}\left(\frac{\eta}{\beta}\right)\right]\right\}}{zq \sinh\left[\text{acosh}\left(\frac{\eta}{\beta}\right)\right]\left(\cosh\left[N\text{acosh}\left(\frac{\eta}{\beta}\right)\right] - \cosh[N\text{acosh}(\eta)]\right)}, \qquad (18)$$

where sgn(n) is the signum function, defined as sgn(n) = -1 when $n < 0$, sgn(n) = 1 when $n > 0$, and sgn(n) = 0 when $n = 0$.

Equations (16), (17), and (18) are not known in the literature, even though expressions similar to Eqs. (16) and (17) can be found in Refs. [35,36], where the continuous time BLRW was derived using an alternative procedure. This procedure

was also used in Ref. [32] to derive Eqs. (12), (13), and (15), for the discrete time BLRW, but only for the case when $q = 1$, that is an always moving walker.

D. Time-dependent propagators with finite domains

To find the time dependence of the propagators one must evaluate the integral (inverse z transform) $P_{n_0}^{(\gamma)}(n, t) =$

$(2\pi i)^{-1} \oint \widetilde{P}_{n_0}^{(\gamma)}(n, z) z^{-t-1} dz$, with $|z| < 1$ and where the integration contour is counterclockwise. Equivalently, one can find time-dependent solution more directly by solving the matricial Master equation

$$\vec{P}(t+1) = \mathbf{A} \cdot \vec{P}(t), \tag{19}$$

where the tridiagonal matrix $\mathbf{A}$ with perturbed corners is given by

$$\mathbf{A} = \begin{bmatrix} 1 - q + \varepsilon & \frac{q}{2}(1+g) & & & \sigma \\ \frac{p}{2}(1-g) & 1-q & \ddots & & \\ & \frac{q}{2}(1-g) & \ddots & \frac{q}{2}(1+g) & \\ & & \ddots & 1-q & \frac{q}{2}(1+g) \\ \nu & & & \frac{q}{2}(1-g) & 1-q+\delta \end{bmatrix}. \tag{20}$$

The different types of boundary conditions are accounted for by a relevant size of $\mathbf{A}$ and appropriately chosen parameters $\varepsilon, \delta, \sigma$ and ν: Reflective boundaries with $\varepsilon = \frac{q}{2}(1+g)$, $\delta = \frac{q}{2}(1-g)$, $\nu = \sigma = 0$ and $\mathbf{A}_{N \times N}$; absorbing boundaries with $\varepsilon = \delta = \nu = \sigma = 0$ and $\mathbf{A}_{(N-2) \times (N-2)}$; mixed boundaries with $\varepsilon = \frac{q}{2}(1+g)$, $\delta = \nu = \sigma = 0$ and $\mathbf{A}_{(N-1) \times (N-1)}$; and periodic boundaries with $\nu = \frac{q}{2}(1+g)$, $\sigma = \frac{q}{2}(1-g)$, $\varepsilon = \delta = 0$ and $\mathbf{A}_{N \times N}$. By diagonalizing the matrix $\mathbf{A}$, the solution can be written as $\vec{P}(t) = \mathbf{L}\mathbf{E}^t\mathbf{R}\vec{P}(0)$ where, respectively, $\mathbf{L}$ and $\mathbf{R}$ are matrices containing the left and right normalized eigenvectors, while $\mathbf{E}$ is the diagonal matrix of eigenvalues. The spatial dependence is determined by the eigenvectors while the eigenvalues give the time dependence. These eigenvalues and eigenvectors are known explicitly for the absorbing, reflecting and periodic cases [37–39], while for the mixed boundary condition we exploit the properties of Chebyshev polynomials to write a propagator with time-dependent coefficients known numerically (see Appendix B for details). To represent the time-dependent propagator a convenient notation is

$$P_{n_0}^{(\gamma)}(n, t) = \sum_{k=w^{(\gamma)}}^{W^{(\gamma)}} h_k^{(\gamma)}(n, n_0)\left[1 + s_k^{(\gamma)}\right]^t, \tag{21}$$

where $w^{(p)} = 0$ and $W^{(p)} = N - 1$ for the periodic case; $w^{(r)} = 0$ and $W^{(r)} = N - 1$ for the reflecting case; $w^{(a)} = 1$ and $W^{(a)} = N - 2$ for the absorbing case; and $w^{(m)} = 1$ and $W^{(m)} = N - 1$ for the mixed case. The time dependence is defined by $[1 + s_k^{(\gamma)}]^t$ with

$$s_k^{(\gamma)} = \begin{cases} q\cos\left(\frac{2k\pi}{N}\right) + iqg\sin\left(\frac{2k\pi}{N}\right) - q, & \gamma = p, \\ \frac{q}{\eta}\cos\left(\frac{k\pi}{N-1}\right) - q, & \gamma = a, \\ \frac{q}{\eta}\cos(\theta_k) - q, & \gamma = m, \\ \begin{aligned} \frac{q}{\eta}\cos\left(\frac{k\pi}{N}\right) - q, & \quad k \neq 0, \\ 0, & \quad k = 0, \end{aligned} & \gamma = r, \end{cases} \tag{22}$$

where $\cos(\theta_k)$ is the kth root of the orthogonal polynomial $f^{\frac{1}{2}}U_{N-1}[\cos(\theta)] - U_{N-2}[\cos(\theta)]$ and where U_n is an nth order Chebyshev polynomial of the second kind. The spatial dependence in Eq. (21) is

$$h_k^{(\gamma)}(n, n_0) = \begin{cases} \dfrac{\exp\left[\frac{2k\pi i(n-n_0)}{N}\right]}{N}, & \gamma = p, \\[2ex] \dfrac{2f^{\frac{n-n_0}{2}}\sin\left[\left(\frac{n-1}{N-1}\right)k\pi\right]\sin\left[\left(\frac{n_0-1}{N-1}\right)k\pi\right]}{N-1}, & \gamma = a, \\[2ex] \dfrac{2f^{\frac{n-n_0}{2}}\sin[(N-n_>)\theta_k]\{f^{\frac{1}{2}}\sin[n_<\theta_k] - \sin[(n_<-1)\theta_k]\}}{(N-1)\cos[(N-1)\theta_k] - Nf^{\frac{1}{2}}\cos[N\theta_k]}, & \gamma = m, \\[2ex] \begin{aligned} \dfrac{f^{\frac{n-n_0-1}{2}}\left\{f^{\frac{1}{2}}\sin\left[\frac{nk\pi}{N}\right] - \sin\left[(n-1)\frac{k\pi}{N}\right]\right\}\left\{f^{\frac{1}{2}}\sin\left[\frac{n_0k\pi}{N}\right] - \sin\left[(n_0-1)\frac{k\pi}{N}\right]\right\}}{N\left(\eta - \cos\left[\frac{k\pi}{N}\right]\right)}, & k \neq 0, \\ \dfrac{f^{n-1}(1-f)}{1-f^N}, & k = 0, \end{aligned} & \gamma = r. \end{cases} \tag{23}$$

In the periodic case, $h_k^{(p)}(n, n_0)$ and $s_k^{(p)}$ are both complex, but Eq. (21) is real. When $g = 0$, $s_k^{(p)}$ becomes real and $h_k^{(p)}(n, n_0) = \cos\left[\frac{2k\pi(n-n_0)}{N}\right]$ because the sin terms cancels out.

In Fig. 2, we plot the propagator in Eq. (21) with two absorbing boundaries ($\gamma = a$) at $n = 1$ and at $n = N$ and with

a negative bias, $g = -0.3$. The drift to the right is evident from the movement of the peak of the probability, while the broadening of the overall shape is due to diffusion.

Using the 1D propagators in Eq. (21) it is possible to recover known solutions to the bounded drift-diffusion equation. In Appendix C we outline the limiting procedure to

obtain the continuous space-time propagators for the four boundary conditions studied.

III. FIRST-PASSAGE PROCESSES IN ONE DIMENSION

An important quantity in transport calculations, already introduced in Sec. II C, is the first-passage probability, $F_{n_0}(n, t)$, to reach a target site n from site n_0 at time t [40]. It is directly related to the propagator through the renewal relation in z-domain $\widetilde{F}_{n_0}(n, z) = \widetilde{P}_{n_0}(n, z)/\widetilde{P}_n(n, z)$. We consider first the reflective domains and subsequently the periodic domain. Using the propagator Eq. (16), the generating function of the first-passage probability is written in a compact manner [see Eq. (D1)] by considering the case when $n > n_0$ and vice versa. Through a z-inversion the time-dependent first-passage probability can be written as

$$F_{n_0}^{(r)}(n, t) = \frac{q f^{\frac{n-n_0}{2}}}{\eta} \begin{cases} \sum_{k=1}^{n-1} \frac{\sin(\theta_k)\left\{ f^{\frac{1}{2}} \sin(n_0\theta_k) - \sin[(n_0-1)\theta_k] \right\} \left[1 - p + \frac{p}{\eta}\cos(\theta_k) \right]^{t-1}}{(n-1)\cos[(n-1)\theta_k] - f^{\frac{1}{2}} n \cos(n\theta_k)} & n > n_0, \\ \sum_{k=1}^{N-n} \frac{\sin(\psi_k)\left(f^{\frac{1}{2}} \sin[(N-n_0)\psi_k] - \sin[(N+1-n_0)\psi_k] \right) \left[1 - p + \frac{p}{\eta}\cos(\psi_k) \right]^{t-1}}{(N+1-n)\cos[(N+1-n)\psi_k] - f^{\frac{1}{2}}(N-n)\cos[(N-n)\psi_k]} & n < n_0 \end{cases} \tag{24}$$

with $F_{n_0}^{(r)}(n, 0) = 0$, and where $\cos(\theta_k)$ and $\cos(\psi_k)$ are, respectively, the kth roots of the orthogonal polynomial $f^{\frac{1}{2}} U_{n-1}[\cos(\theta_k)] - U_{n-2}[\cos(\theta_k)]$ and $f^{\frac{1}{2}} U_{N-1-n}[\cos(\psi_k)] - U_{N-n}[\cos(\psi_k)]$ with $U_{-1} = 0$

For the periodic case a similar procedure gives a compact expression in Eq. (D2) by treating $n > n_0$ and $n < n_0$ separately. Using the signum function the time dependence can be written conveniently as the following single expression:

$$F_{n_0}^{(p)}(n, t) = \frac{q f^{\frac{n-n_0}{2}}}{\eta N} \sum_{k=1}^{N-1} (-1)^{k+1} \sin\left(\frac{k\pi}{N}\right) \left\{ \sin\left[(N - |n - n_0|) \frac{k\pi}{N} \right] + \sin\left[|n - n_0| \frac{k\pi}{N} \right] f^{-\frac{N \mathrm{sgn}(n-n_0)}{2}} \right\} \left[1 - q + \frac{q}{\eta} \cos\left(\frac{k\pi}{N}\right) \right]^{t-1}, \tag{25}$$

with $F_{n_0}^{(p)}(n, 0) = 0$.

In the case of periodic domains, an interesting feature is the appearance of two peaks in the first-passage probability. While the first-passage dynamics of a diffusive walker in a periodic domain is monomodal, in the presence of a bias one can find bimodal features. To display these features we plot $F_{n_0}^{(p)}(n, t)$ in Fig. 3. Figures 3(a)–3(d) depict the first-passage probability to the same target at $n = 4$ starting from $n_0 = 2$ but each panel represents a stronger bias from left to right.
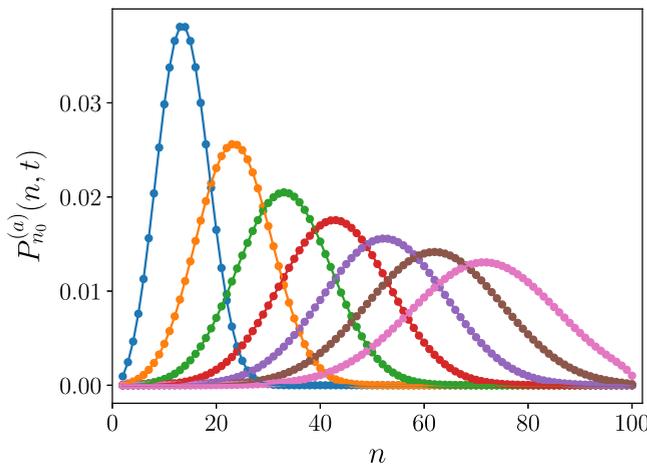
FIG. 2. One-dimensional propagator with absorbing boundaries at sites 1 and 101. The localized initial condition is at $n_0 = 2$ and the bias and diffusive parameters are, respectively, $g = -0.3$ and $q = 0.8$. Each of the curves represent the probability at different times, with the left most curve being at $t = 40$, the right most being at $t = 280$ and $\Delta t = 40$ between each of them. The dots are from Eq. (21) with $\gamma = a$, whereas the solid lines are obtained by solving iteratively Eq. (19).

Figures 3(e)–3(h) have the same bias, $g = 0.35$, but the target locations are displaced away from the starting site $n_0 = 2$. In the absence of a bias, i.e., Fig. 3(a), one finds a monomodal probability function characteristic of diffusive processes. As the bias is increased to positive values (first row), the walker is more likely to travel leftwards taking the longer route to reach the target (via the site N) resulting in the appearance of a second peak and at the same time the gradual loss of the first. In the left ballistic limit, one expects the first peak to be completely lost and the second peak to be a Kronecker δ at $N - n + n_0$ [see Eqs. (D4) and (D5) in Appendix D for the limiting expressions of Eq. (25) when $f \to 0$ and $f \to \infty$]. With the bias fixed (second row), as one moves the target site further away from n_0 and opposite to the direction of the bias, the first peak is gradually lost while the second becomes more prominent. With the target site close to n_0, the distance to travel against the bias to reach n is small enough such that there is still a high probability of reaching n from n_0 without visiting N. As one increases the distance between n_0 and n, with $n > n_0$, the likelihood of a walker traveling this distance against the bias decreases resulting in the progressive loss of the first peak.

A. Mean first-passage time

By using the first-passage generating function with reflecting or periodic boundaries, in Eq. (D1) or Eq. (D2) in Appendix D, one finds the mean of the probability through $T_{n_0 \to n}^{(\gamma)} = \frac{d}{dz} \widetilde{F}_{n_0}^{(\gamma)}(n, z)|_{z \to 1}$, to give the MFPT,

$$T_{n_0 \to n}^{(r)} = \frac{1}{q} \frac{(f+1)}{(f-1)^2} \{ (n - n_0)(f - 1)$$
$$+ f^{\frac{N}{2}[1 - \mathrm{sgn}(n-n_0)]} (f^{1-n} - f^{1-n_0}) \} \tag{26}$$
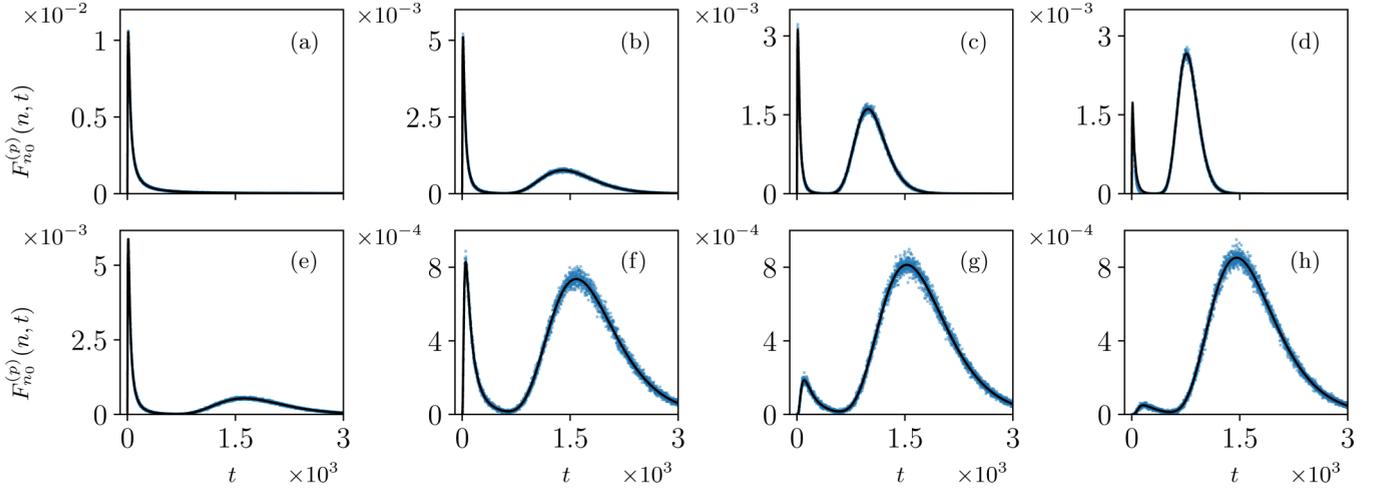
FIG. 3. First-passage probability of a 1D random walk with bias in a periodic domain with $N = 50$ sites, initial position $n_0 = 2$, and diffusive parameter $q = 0.1$. Panels (a)–(d) all have the target at site $n = 4$, but differ in the bias which is, respectively, $g = 0, 0.3, 0.45$, and 0.6. The panels (e), (f) have the same bias, $g = 0.35$, while differing in the position of the target site, which is $n = 4, 6, 8$ and 10, respectively. The solid black line is from Eq. (25), whereas the blue circles are from 10^6 stochastic simulations.

and

$$T_{n_0 \to n}^{(p)} = \frac{1}{q} \frac{(f+1)}{(f-1)(f^N-1)} \{(n-n_0)(f^N - 1)$$
$$+ N f^{\frac{N}{2}[1-\text{sgn}(n-n_0)]}(1 - f^{n-n_0})\}. \quad (27)$$

In the left (right) ballistic limit, that is $q \to 1$ and $f \to 0$ ($f \to \infty$) of Eq. (26), we find the MFPT to be $|n - n_0|$ if the target is in the direction of the bias or infinite if the target is against the bias. However, the MFPT with periodic boundaries in Eq. (27) will always be finite: With $n > n_0$ in the left ballistic limit $T_{n_0 \to n}^{(p)} = N - |n - n_0|$, while in the right ballistic limit $T_{n_0 \to n}^{(p)} = |n - n_0|$ and vice versa. In the diffusive limit, i.e., $f \to 1$, Eqs. (26) and (27) reduce to [22]

$$T_{n_0 \to n}^{(r)} = \frac{1}{q}[N|n - n_0| + (n - n_0)(n + n_0 - 1 - N)]$$

and

$$T_{n_0 \to n}^{(p)} = \frac{1}{q}(N - |n - n_0|)|n - n_0|,$$

respectively.

IV. DYNAMICS IN HIGHER DIMENSIONS

To find propagators in higher dimensions we need both the series solution and the compact solution from the method of images. The procedure for finding propagators in higher dimension is a slight variation of the eight-step method introduced by one of the present authors [22]. To illustrate this new procedure we first present the case of a walker in a 2D domain with reflective boundary conditions.

A. Two-dimensional propagator with reflective boundaries

We start by considering the dynamics of a walker on a 2D lattice that is bounded along the first dimension whilst unbounded in the second. The probability of stepping left or right along the first dimension are, respectively, $\frac{q_1}{4}(1 - g_1)$ or

$\frac{q_1}{4}(1 + g_1)$. Similarly stepping left or right along the second dimension are, respectively, $\frac{q_2}{4}(1 - g_2)$ or $\frac{q_2}{4}(1 + g_2)$. In the bulk of the domain, the probability of remaining at a site is $1 - \frac{q_1}{2} - \frac{q_2}{2}$, while along the left (or right) boundary at $n_1 = 1$ (or at $n_1 = N_1$), is $1 - \frac{q_1}{4}(1 - g_1) - \frac{q_2}{2}$ (or $1 - \frac{q_1}{4}(1 + g_1) - \frac{q_2}{2}$). The dynamics in the bulk of the domain are governed by the Master equation

$$P(n_1, n_2, t + 1)$$
$$= \left[1 - \frac{q_1}{2} - \frac{q_2}{2}\right] P(n_1, n_2, t)$$
$$+ \frac{q_1}{4}[(1 - g_1)P(n_1 - 1, n_2, t) + (1 + g_1)P(n_1 + 1, n_2, t)]$$
$$+ \frac{q_2}{4}[(1 - g_2)P(n_1, n_2 - 1, t) + (1 + g_2)P(n_1, n_2 + 1, t)], \quad (28)$$

along the left boundary by

$$P(1, n_2, t + 1)$$
$$= \left[1 - \frac{q_1}{4}(1 - g_1) - \frac{q_2}{2}\right] P(1, n_2, t)$$
$$+ \frac{q_2}{4}[(1 - g_2)P(1, n_2 - 1, t) + (1 + g_2)P(1, n_2 + 1, t)]$$
$$+ \frac{q_1}{4}(1 + g_1)P(2, n_2, t), \quad (29)$$

and along the right boundary by

$$P(N_1, n_2, t + 1)$$
$$= \left[1 - \frac{q_1}{4}(1 + g_1) - \frac{q_2}{2}\right] P(N_1, n_2, t)$$
$$+ \frac{q_2}{4}[(1 - g_2)P(1, n_2 - 1, t) + (1 + g_2)P(1, n_2 + 1, t)]$$
$$+ \frac{q_1}{4}(1 - g_1)P(N_1 - 1, n_2, t), \quad (30)$$

Note that $\sum_{n_1=1}^{N_1} \sum_{n_2=1}^{N_2} P(n_1, n_2, t+1) = \sum_{n_1=1}^{N_1} \sum_{n_2=1}^{N_2} P(n_1, n_2, t)$, which indicates that Eqs. (28), (29), and (30) represent a probability preserving Master equation.

Symmetrizing the dynamics and Fourier transforming along the second dimension results in an effective 1D problem, analogous to Eq. (19),

$$\widehat{Q}(n_1, \kappa_2, t+1) = \sum_{\ell=1}^{N_1} \mathbf{B}_{n_1,\ell} \, \widehat{Q}(\ell, \kappa_2, t), \qquad (31)$$

where $\mathbf{B}$ is a tridiagonal matrix with elements on the upper and lower diagonal being, respectively, $\frac{\omega q_1}{2}(1 + g_1)$ and $\frac{\omega q_1}{2}(1 - g_1)$ with $\omega^{-1} = 1 - \frac{q_2}{2} + \frac{q_2}{2\eta_2}$. The elements along the diagonal are $B_{\ell,\ell} = \omega[1 - \frac{q_1}{2} - \frac{q_2}{2} + \frac{q_2}{\eta_2} \cos(\kappa_2)]$, when $\ell \neq 1, N_1$, $\quad B_{1,1} = \omega[1 - \frac{q_1}{4}(1 - g_1) - \frac{q_2}{2} + \frac{q_2}{\eta_2} \cos(\kappa_2)]$, $B_{N_1,N_1} = \omega[1 - \frac{q_1}{4}(1 + g_1) - \frac{q_2}{2} + \frac{q_2}{\eta_2} \cos(\kappa_2)]$. After supplementing the initial conditions $\widehat{Q}(n_1, \kappa_2, 0) = \delta_{n_1, n_{0_1}} e^{-i\kappa_2 n_{0_2}} f_2^{-\frac{n_{0_2}}{2}} (1 - f_2^{-1})$, Eq. (31), due to the comparable structure with Eq. (19), can be solved explicitly in z and Fourier domains. Subsequently, inverse Fourier transforming the second dimension, applying the method of images, reversing to the asymmetric propagator and finally, after inverse z transforming, one obtains the exact spatiotemporal dependence (the calculation is outlined in Appendix E). Knowledge of the identity Eq. (G1), allows us to write the time-dependent solution to the 2D random walks with independent bias in each dimension as

$$P_{\vec{n}_0}^{(r_1, r_1)}(n_1, n_2, t)$$
$$= \lambda_1 \lambda_2 + \sum_{k_1=1}^{N_1-1} \sum_{k_2=1}^{N_2-1} h_{k_1}^{(r_1)}(n_1, n_{0_1}) h_{k_2}^{(r_2)}(n_2, n_{0_2})$$
$$\times \left[1 + \frac{s_{k_1}^{(r_1)}}{2} + \frac{s_{k_2}^{(r_2)}}{2} \right]^t$$
$$+ \lambda_1 \sum_{k_2=1}^{N_2-1} h_{k_2}^{(r_2)}(n_2, n_{0_2}) \left[1 + \frac{s_{k_2}^{(r_2)}}{2} \right]^t$$
$$+ \lambda_2 \sum_{k_1=1}^{N_1-1} h_{k_1}^{(r_1)}(n_1, n_{0_1}) \left[1 + \frac{s_{k_1}^{(r_1)}}{2} \right]^t, \qquad (32)$$

where

$$\lambda_i = \frac{f_i^{n_i-1}(1 - f_i)}{1 - f_i^{N_i}}.$$

A similar procedure can be applied for the case of the absorbing, periodic, and mixed boundary conditions, although in the latter case, as mentioned earlier, the analytic solution is not fully explicit, but based on the numerical roots of the orthogonal polynomials of the form $f^{\frac{1}{2}} U_{s-1}(x) - U_{s-2}(x)$.

In Fig. 4, we plot $P_{\vec{n}_0}^{(r_1, r_2)}(n_1, n_2, t)$ for a specific time value with the left-downward bias $\vec{g} = (0.1, 0.1)$. A feature worth pointing out is the appearance of two saddle points that emerge at intermediate times. They appear due to the steady-state probability at the boundary being higher than the
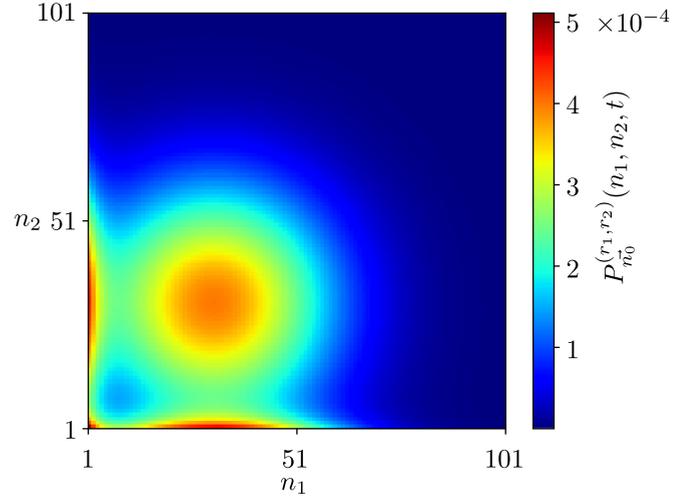
FIG. 4. Two-dimensional propagator, from Eq. (32), evaluated at $t = 10^3$ with a domain of size $\vec{N} = (101, 101)$. The initial condition is $\vec{n} = (71, 71)$, the diffusion parameters are $\vec{q} = (0.8, 0.8)$ and the bias parameters are $\vec{g} = (0.1, 0.1)$.

transient peak. In 1D this results in the appearance of a local minimum.

B. Propagator in arbitrary dimensions and arbitrary boundary conditions

We use a hierarchical procedure to contruct bias lattice walk propagators of any dimensions by generalizing the procedure used to derive the 2D random walk propagator Eq. (32) (the summary of the procedure can be found in Appendix F). The resulting analytic propagators are

$$P_{\vec{n}_0}^{(\vec{\gamma})}(\vec{n}, t) = \sum_{k_1=w^{(\gamma_1)}}^{W^{(\gamma_1)}} \cdots \sum_{k_d=w^{(\gamma_d)}}^{W^{(\gamma_d)}} \prod_{j=1}^{d} h_{k_j}^{(\gamma_j)}(n_j, n_{0_j})$$
$$\times \left[1 + \frac{s_{k_1}^{(\gamma_1)}}{d} + \cdots + \frac{s_{k_d}^{(\gamma_d)}}{d} \right]^t, \qquad (33)$$

with $s_k^{(\gamma)}$ and $h_k^{(\gamma)}(n, n_0)$ defined, respectively, in Eqs. (22) and (23), and with $\omega^{(\gamma)}$ and $W^{(\gamma)}$ defined after Eq. (21). Using Eq. (33), one can derive first-passage (or first-return) probability and mean-first passage times in higher dimensions with an abitrary combination of reflecting and periodic boundaries which were previously unknown. Such expressions enable one to study transport process that were, until now, only possible through numerical means. In the following subsections we employ Eq. (33) to reveal an intricate bias depedence on the time-dependent first-return probability, and we study the effect of bias on the mean first-passage times in a multitarget environment.

1. First-return processes in higher dimensions

A useful quantity in studying search processes is the probability of the first recurrence of an event, that is the probability of a lattice walker returning to the starting location for the first time. The first-return probability, or henceforth, the return probability, is derived via the renewal equation and in
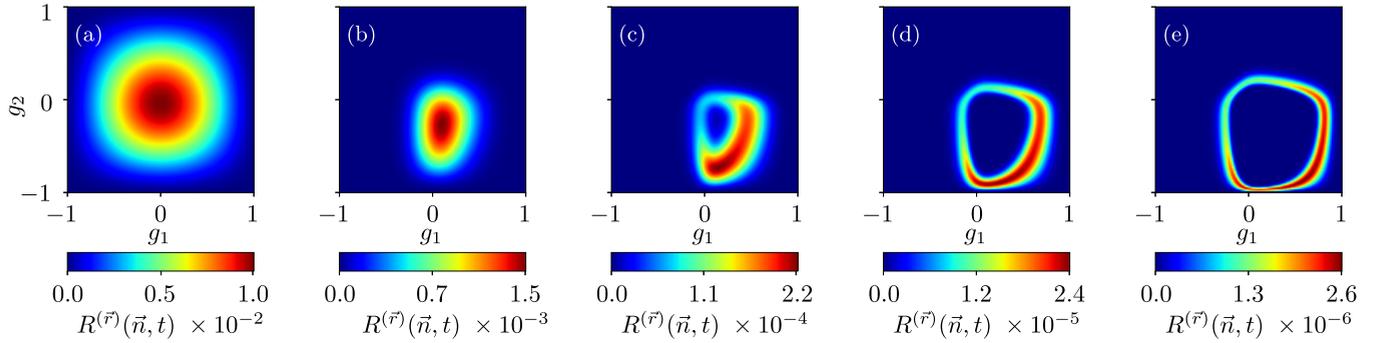
FIG. 5. Return probability to the site $\vec{n} = (5, 18)$ as a function of the bias $\vec{g}$ for a 2D BLRW with reflecting boundaries. We use a domain of size $\vec{N} = (20, 20)$ and a diffusion parameter of value $\vec{q} = (0.8, 0.8)$. A positive (negative) g_1 indicates a drift to the left (right), while a positive (negative) g_2 indicates a drift downwards (upwards). The panels (a) to (e) represent, respectively, $R^{(r)}(n, t)$ at time $t = 10, 10^2, 10^3, 10^4$, and 10^5.

z-domain it is given by $\widetilde{R}^{(\vec{r})}(\vec{n}, z) = 1 - [\widetilde{P}_{\vec{n}}^{(r)}(\vec{n}, z)]^{-1}$. The study of the return probability on lattice random walks has a long history [41,42]. Used originally for unbounded d-dimensional lattices where it is found that a walker returns with certainty to the starting location in 1D and 2D while for higher dimensions there is a finite probability that the walker does not return. Although the walker is bound to return to its initial position in unbounded 1D and 2D domains, the mean return time (MRT) is always infinite. In bounded domains, however, the MRT is finite and is equal to the reciprocal of the steady-state probability at the site [19]. For a LRW (without bias) the steady-state probability is uniform and the MRT reduces to the domain size. In the presence of a non uniform steady state, as is the case with BLRW with reflecting boundaries, the MRT, $\mathcal{R}_{\vec{n}}^{(\vec{r})}$, becomes site-dependent and the return dynamics may be rather complex. Namely, given an off-centre lattice site, one finds the MRT to be minimized for a bias with a specific direction (see Appendix H).

However, the MRT may hide the nuances of the temporal dynamics. To examine these dynamics, we use the starting location $\vec{n} = (5, 18)$, and track the return probability, $R^{(\vec{r})}(\vec{n}, t)$, at different times. We do this in Fig. 5 by plotting $R^{(\vec{r})}(\vec{n}, t)$ as a function $\vec{g}$. We use known numerical methods [43] to invert the generating function and plot in each panel the return probability for progressively longer times from Fig. 5(a) to 5(e).

At short times [Fig. 5(a)] one finds the return probability to be independent of the bias direction as any bias pushes the

walker away from the starting location lowering the likelihood of return. With $t = 10^2$ in Fig. 5(b) we observe greater return probabilities for certain values of $g_1 > 0$ and $g_2 < 0$. Since the time t is comparable to the shortest MRT (see Appendix H), one expects the likelihood of returning at $t = 10^2$ to be greater for the bias that yields the shortest MRT. A further increase in time ($t = 10^3$) results in the appearance of a void. The void represents an area around a local minimum of $R^{(\vec{r})}(\vec{n}, t)$. Its appearance indicates that a large number of the trajectories for which the bias has values inside, have already returned when compared to those with bias outside of the void. We thus observe an arched area of high return probability in Fig. 5(c) compared to the area around a maximum in Fig. 5(b). Increasing time further in Figs. 5(d) and 5(e) results in the expansion of the void as stronger biases are necessary to increase the probability of returning at longer times. One also observes the radial stretching of the area of high return probability as the dependence on the bias direction is progressively lost. In the limit of large time the high values of $R^{(\vec{r})}(\vec{n}, t)$ acquires a square shape close to the extreme values of $\vec{g}$, namely, $(-1, -1)$, $(-1, 1)$, $(1, 1)$, and $(1, -1)$.

2. First-passage processes in higher dimensions

Using the z transform of Eq. (33) one can show that the MFPT in higher dimensions with either reflective, periodic or a mixture of the two types of boundaries, is given by

$$T_{\vec{n}_0 \to \vec{n}}^{(\vec{\gamma})} = \frac{d}{\Omega} \sum_{\substack{k_1=0 \\ k_1+\cdots+k_d>0}}^{W^{(\gamma_1)}} \cdots \sum_{k_d=0}^{W^{(\gamma_1)}} \frac{h_{k_1}^{(\gamma_1)}(n_1, n_{0_d}) \cdots h_{k_d}^{(\gamma_d)}(n_d, n_{0_d}) - h_{k_1}^{(\gamma_1)}(n_1, n_1) \cdots h_{k_1}^{(\gamma_d)}(n_d, n_d)}{s_{k_1}^{(\gamma_1)} + \cdots + s_{k_d}^{(\gamma_d)}}, \tag{34}$$

where $\Omega = \prod_{j=1}^{d} h_0^{(\gamma_j)}(n_j, n_{0_j})$, which is dependent only on n_j when $\gamma = r$, and is independent of n_j and n_{0_j} when $\gamma = p$; where $s_k^{(\gamma)}$ and $h_k^{(\gamma)}(n, n_0)$ are defined, respectively, in Eqs. (22) and (23); and with $W^{(\gamma)}$ defined after Eq. (21).

The first-passage dynamics becomes very rich in the presence of multiple targets as the bias toward a specific target

influences dramatically the time it takes to reach either of the targets. We show this dependence by plotting in Fig. 6 the MFPT to either of three targets as a function of the position of the first target in a 2D box with reflective boundaries. We use Eq. (34) and the MFPT expression to either of three targets from Ref. [22]. Figure 6(a) depicts the schematic
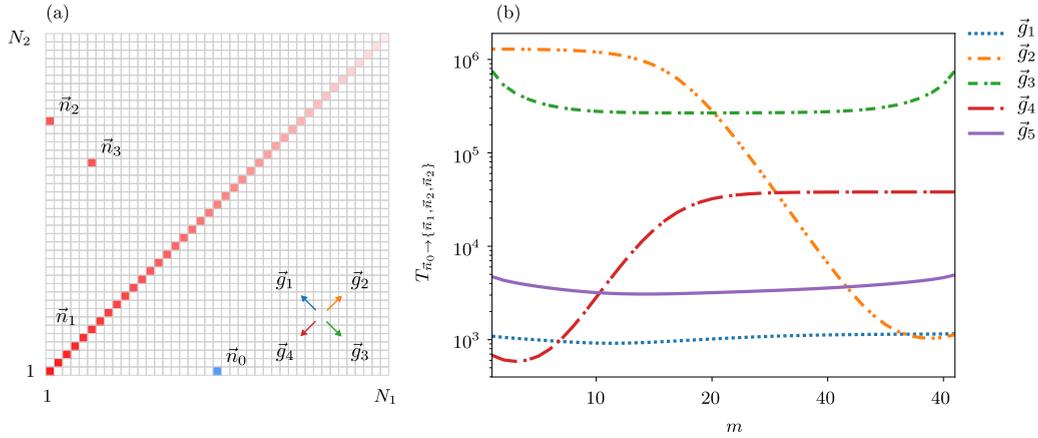
FIG. 6. MFPT in a 2D domain of size $\vec{N} = (41, 41)$ with reflective boundary conditions to either of three targets. The walker is initially at $\vec{n}_0 = (21, 1)$ with diffusion parameter $\vec{q} = (0.8, 0.8)$. The coordinates of the first target are $\vec{n}_1 = (m, m)$ with $1 \leqslant m \leqslant 41$, while that of the second and third targets are static with respective positions $\vec{n}_2 = (1, 31)$ and $\vec{n}_3 = (6, 26)$. The different biases considered are $\vec{g}_1 = (0.1, -0.1)$, $\vec{g}_2 = (-0.1, -0.1)$, $\vec{g}_3 = (-0.1, 0.1)$, $\vec{g}_4 = (0.1, 0.1)$ and the fully diffusive case $\vec{g}_5 = (0, 0)$. Panel (a) shows a schematic diagram of the setup with the positions of the targets, the initial condition and the directions of the different biases. In panel (b) for each bias we plot the MFPT as a function of the position of the third target.

diagram of the lattice, the biases and the position of the targets. The position of the targets $\vec{n}_2$ and $\vec{n}_3$ are fixed while the position of the first target $\vec{n}_1 = (m, m)$ is slid along the diagonal.

The bias $\vec{g}_1$ shows the least dependence on the position of the first target. With the bias $\vec{g}_1$, the walker always has a high probability of reaching the second or third target regardless of the position of the first. The shorter MFPT in this case occurs when the line connecting $\vec{n}_0$ to $\vec{n}_1$ is parallel to $\vec{g}_1$, i.e., when $m = 11$. The diffusive case, $\vec{g}_5$, shows a slightly stronger dependence on m than $\vec{g}_1$, with its shortest MFPT value being attributed to when the first target is closer to $\vec{n}_0$, that is when $m = 14$. As the direction of the bias $\vec{g}_3$ is always away from the targets, the MFPT decreases as the first target is moved. It gives the minimum MFPT in correspondence to the shortest distance that the walker travels against the bias to reach $\vec{n}_1$.

With $\vec{g}_2$ and $\vec{g}_4$ being opposite to each other and parallel to any of the positions of the first target, the corresponding MFPT displays similar characteristics. When $m = 1$ ($m = 41$), corresponding with the first target located in the bottom-left (top-right) corner, the bias $\vec{g}_4$ ($\vec{g}_2$) exhibits the shortest MFPT due to the bias pushing trajectories toward the corner. As m is increased from $m = 1$, the MFPT of $\vec{g}_4$ increases due to $\vec{n}_1$ moving out of the bottom-left corner. Analogously, as m is decreased from $m = 41$, $\vec{n}_1$ moves out of the top-right corner causing the MFPT of $\vec{g}_2$ to increase. The difference in the high values of the MFPT of $\vec{g}_4$ when $m > 30$, and the MFPT of $\vec{g}_2$ when $m < 10$, is due to the position of the second and third targets. With $\vec{n}_2$ and $\vec{n}_3$ being closer to the bottom-left than the top-right corner, one expects the largest MFPT of $\vec{g}_4$ to be smaller than the largest MFPT of $\vec{g}_2$, and vice versa for the shortest MFPT.

An interesting observation is that when the first target is positioned in the top-right corner with $m > 35$, the MFPT of $\vec{g}_2$ and $\vec{g}_1$ are comparable. It highlights the strong dependence of the MFPT on the positioning of the targets relative to the

boundary corner. In the presence of a bias, one can achieve shorter or similar MFPTs by positioning fewer targets close to the corner and in the direction of the bias ($\vec{g}_2$ case with high m) as opposed to many targets away from it ($\vec{g}_1$ case).

Our observations are particularly relevent in the domain of field-driven translocation in channels with periodic corrugation. Here, one is interested in the first-passage times of tracer particle moving under an external bias. Recent numerical analysis [31] reveals that particles travel close to the boundaries as they pass through a funnel. For further work, it would be interesting to reaffirm such results, by studying the MFPT using a similar setup to Fig. 6(a), but with targets concentrated in the corner and by changing the initial position instead of a target position. With the two orthogonal boundaries acting like a funnel one expects similar results to those observed numerically.

V. CONCLUSIONS

We conclude, by reminding that while the continuous-time BLRW in confined domains has been studied extensively in 1D [35,36], a thorough treatment of the analogous discrete time case was missing from the literature and only the propagator for the case $q = 1$ and with absorbing boundaries was known [32]. Compared to Ref. [32], here we have derived the generating function of the 1D propagator in finite domains by employing an alternative procedure yielding both finite series and compact expressions, with the latter used to create the generating function for the first-passage probability in reflecting and periodic domains. To find the time-dependent propagators, we have used known results for tridiagonal matrices with perturbed corners [39,44] instead of inverting the generating function of the propagators via a contour integral. From the finite series time-dependent propagators we have recovered the known solutions to the drift-diffusion equation, linking the movement parameters of a BLRW with the

drift velocity and the diffusion coefficient for a Brownian walker.

By exploiting the properties of Chebyshev polynomials, the generating function of the first-passage probability with periodic and reflective boundaries was inverted explicitly to yield the exact time dependence. Surprisingly, the periodic case was shown to display bimodal features when its analog without bias is known to be monomodal. Last, by employing a hierarchical-dimensional reduction we have derived time-dependent propagators for the confined BLRW in any number of dimensions and with arbitrary boundary conditions. The propagators were then used to find explicit expressions for the mean first-passage time in a d-dimensional box, torus or an arbitrary combination of both. The generating function of the propagators have also highlighted the influence a bias may have on the time dependence of the return probability.

APPENDIX A: DERIVATION OF PROPAGATORS IN 1D WITH REFLECTIVE BOUNDARIES

1. Single reflective boundary

The Kronecker δ initial condition for the propagator $\mathcal{P}_{n_0}^{(r)}(n,0) = \delta_{n,n_0}$ gives an initial condition for the symmetric propagator with $\mu = f^{-\frac{1}{2}}$ in Eq. (4) equal to $\mathcal{Q}^{(a)}(n,0) = f^{-\frac{n}{2}}\delta_{n,n_0} - f^{-\frac{n+2}{2}}\delta_{n+1,n_0}$. Convoluting this initial condition with the symmetric propagator (9) and accounting for the contribution of the image of the initial condition via $\widetilde{\mathcal{Q}}^{(a)}(n,z) = \sum_{m=0}^{\infty} \mathcal{Q}^{(a)}(m,0)[\widetilde{H}_m(n,z) - \widetilde{H}_{-m}(n,z)]$ gives

$$\widetilde{\mathcal{Q}}^{(a)}(n,z) = \frac{\varphi^{-|n-n_0|} - \varphi^{-|n+n_0|}}{[1-z\omega(1-q)]\sqrt{1-\zeta^2}} - \frac{f^{-\frac{1}{2}}(\varphi^{-|n-n_0+1|} - \varphi^{-|n+n_0-1|})}{[1-z\omega(1-q)]\sqrt{1-\zeta^2}}, \tag{A1}$$

where ζ and φ are defined in Eq. (10) and Eq. (11), respectively. Using Eq. (A1) in Eq. (7) yields

$$\widetilde{\mathcal{P}}_{n_0}^{(r)}(n,z) = \frac{1}{[1-z(1-q)]\sqrt{1-\left(\frac{\beta}{\eta}\right)^2}} \sum_{j=0}^{\infty} f^{-\frac{j}{2}}(\alpha^{-|n-n_0+j|} - \alpha^{-|n+n_0+j|}) - f^{-\frac{j+1}{2}}(\alpha^{-|n-n_0+j+1|} - \alpha^{-|n+n_0+j-1|}). \tag{A2}$$

To assist in evaluating Eq. (A2), it is useful to consider the full summation as differences of two series. The difference involving $\alpha^{-|n-n_0|}$ terms produces

$$\sum_{j=0}^{\infty} f^{-\frac{j}{2}}\alpha^{-|n-n_0+j|} - \sum_{j=0}^{\infty} f^{-\frac{j+1}{2}}\alpha^{-|n-n_0+j+1|} = \alpha^{-|n-n_0|}, \tag{A3}$$

as the only surviving term is the $j = 0$ term, whereas evaluating the sum with the terms $\alpha^{-|n+n_0|}$ gives

$$\sum_{j=0}^{\infty} f^{-\frac{j+1}{2}}\alpha^{-|n+n_0+j-1|} - \sum_{j=0}^{\infty} f^{-\frac{j}{2}}\alpha^{-|n+n_0+j|} = \frac{\alpha^{-|n+n_0|}(\alpha - f^{\frac{1}{2}})}{f^{\frac{1}{2}} - \alpha^{-1}}. \tag{A4}$$

Hence, the propagator with a single reflective boundary between the sites $n = 0$ and $n = 1$ in z-domain is

$$\widetilde{\mathcal{P}}_{n_0}^{(r)}(n,z) = \frac{1}{[1-z(1-q)]\sqrt{1-\zeta^2}}\left[\alpha^{-|n-n_0|} + \frac{\alpha^{-|n+n_0|}(\alpha - f^{\frac{1}{2}})}{f^{\frac{1}{2}} - \alpha^{-1}}\right]. \tag{A5}$$

With some simple algebra one then obtains Eq. (13) in the main text.

2. Two reflective boundaries

With the domain being finite, one must construct the bounded propagator with an infinite number of images of the propagator Eq. (9) with shifted initial conditions. Similar to the case with a single reflecting boundary, the initial condition $P_{n_0}^{(r)}(n,0) = \delta_{n,n_0}$ translates into $\mu = f^{-\frac{1}{2}}$ and $Q^{(a)}(n,0) = f^{-\frac{n}{2}}\delta_{n,n_0} - f^{-\frac{n+2}{2}}\delta_{n+1,n_0}$. Convolution of this initial condition with the general solution constructed with infinite images of the unbounded propagator Eq. (9) via $\widetilde{Q}^{(a)}(n,z) = \sum_{m=0}^{N}\sum_{k=-\infty}^{+\infty} Q^{(a)}(m,0)[\widetilde{H}_{m+2kN}(n,z) - \widetilde{H}_{-m+2kN}(n,z)]$ gives

$$\widetilde{Q}^{(a)}(n,z) = \sum_{k=-\infty}^{\infty} \frac{\varphi^{-|n-n_0+2kN|} - \varphi^{-|n+n_0+2kN|}}{[1-z\omega(1-q)]\sqrt{1-\zeta^2}} - f^{-\frac{1}{2}}\sum_{k=-\infty}^{\infty}\frac{\varphi^{-|n-n_0+1+2kN|} - \varphi^{-|n+n_0-1+2kN|}}{[1-z\omega(1-q)]\sqrt{1-\zeta^2}}. \tag{A6}$$

Summing the images yields the solution to the symmetric propagator with absorbing boundaries at $n = 0$ and $n = N$,

$$\widetilde{Q}^{(a)}(n, z) = \frac{\varphi^{N-|n-n_0|} + \varphi^{-N+|n-n_0|} - \varphi^{N-|n+n_0|} - \varphi^{-N+|n+n_0|}}{(\varphi^N - \varphi^{-N})[1 - z\omega(1-q)]\sqrt{1 - \zeta^2}}$$
$$- f^{-\frac{1}{2}} \left\{ \frac{\varphi^{N-|n-n_0+1|} + \varphi^{-N+|n-n_0+1|} - \varphi^{N-|n+n_0-1|} - \varphi^{-N+|n+n_0-1|}}{(\varphi^N - \varphi^{-N})[1 - z\omega(1-q)]\sqrt{1 - \zeta^2}} \right\}. \tag{A7}$$

To transform back to the symmetric propagator we apply the transformation Eq. (7) to Eq. (A7) and we obtain

$$\widetilde{\mathcal{P}}_{n_0}^{(r)}(n, z) = \sum_{j=0}^{\infty} f^{-\frac{j}{2}} \left\{ \frac{\alpha^{N-|n-n_0|} + \alpha^{-N+|n-n_0|} - \alpha^{N-|n+n_0|} - \alpha^{-N+|n+n_0|}}{(\alpha^N - \alpha^{-N})[1 - z(1-q)]\sqrt{1 - \left(\frac{\eta}{\beta}\right)^2}} \right\}$$
$$- \sum_{j=0}^{\infty} f^{-\frac{j+1}{2}} \left\{ \frac{\alpha^{N-|n-n_0+1|} + \alpha^{-N+|n-n_0+1|} - \alpha^{N-|n+n_0-1|} - \alpha^{-N+|n+n_0-1|}}{(\alpha^N - \alpha^{-N})[1 - z(1-q)]\sqrt{1 - \left(\frac{\eta}{\beta}\right)^2}} \right\}. \tag{A8}$$

We proceed in a similar fashion as before by considering pairwise differences of the series. The $\alpha^{\pm N \mp |n-n_0|}$ terms result in the difference of two geometric series, namely,

$$\alpha^{\pm N \mp |n-n_0|} = \sum_{j=0}^{\infty} f^{-\frac{j}{2}} \alpha^{\pm N \mp |n-n_0+j|} - \sum_{j=0}^{\infty} f^{-\frac{j+1}{2}} \alpha^{\pm N \mp |n-n_0+j+1|}, \tag{A9}$$

while the $\alpha^{\pm N \mp |n+n_0|}$ terms produce a difference of the following geometric series

$$\alpha^{\pm N \mp |n+n_0|} \left[\frac{\alpha - f^{\frac{1}{2}}}{f^{\frac{1}{2}} - \alpha^{-1}} \right]^{\pm 1} = \sum_{j=0}^{\infty} f^{-\frac{j+1}{2}} \alpha^{\pm N \mp |n+n_0+j-1|} - \sum_{j=0}^{\infty} f^{-\frac{j}{2}} \alpha^{\pm N \mp |n+n_0+j|}. \tag{A10}$$

Putting everything together we find

$$\widetilde{P}_{n_0}^{(r)}(n, z) = \frac{\eta f^{\frac{n-n_0}{2}}}{zq \sinh\left[\mathrm{acosh}\left(\frac{\eta}{\beta}\right)\right]} \left\{ \frac{\alpha^{N-|n-n_0|} + \alpha^{-N+|n-n_0|} - \alpha^{N-|n+n_0|}\xi - \alpha^{-N+|n+n_0|}\xi^{-1}}{2 \sinh\left[N\mathrm{acosh}\left(\frac{\eta}{\beta}\right)\right]} \right\}, \tag{A11}$$

and with some further algebra we obtain Eq. (16) in the main text.

APPENDIX B: TIME-DEPENDENT SOLUTION WITH MIXED BOUNDARY CONDITION

We rewrite the mixed propagator Eq. (17) in terms of Chebyshev polynomials of the second kind,

$$\widetilde{P}_{n_0}^{(m)}(n, z) = \frac{2\eta f^{\frac{n-n_0}{2}} U_{N-n_>-1}\left(\frac{\eta}{\beta}\right) \left\{ f^{\frac{1}{2}} U_{n_<-1}\left(\frac{\eta}{\beta}\right) - U_{n_<-2}\left(\frac{\eta}{\beta}\right) \right\}}{zq \left\{ f^{\frac{1}{2}} U_{N-1}\left(\frac{\eta}{\beta}\right) - U_{N-2}\left(\frac{\eta}{\beta}\right) \right\}}. \tag{B1}$$

To find the inverse z transform of Eq. (17), we first find the roots of the orthogonal polynomial $f^{\frac{1}{2}} U_{N-1}(\sigma) - U_{N-2}(\sigma)$. Defining $\cos(\theta_k)$ as the roots, the time-dependent solution is then written as

$$2f^{\frac{n-n_0}{2}} \sum_{k=1}^{N-1} \lim_{\sigma \to \cos(\theta_k)} \frac{\left[1 - p + \frac{p}{\eta}\cos(\theta_k)\right]^t [\sigma - \cos(\theta_k)] U_{N-n_>-1}(\sigma) \left\{ f^{\frac{1}{2}} U_{n_<-1}(\sigma) - U_{n_<-2}(\sigma) \right\}}{f^{\frac{1}{2}} U_{N-1}(\sigma) - U_{N-2}(\sigma)}. \tag{B2}$$

To evaluate the limit we apply L'Hôpital's rule [45] to obtain

$$2f^{\frac{n-n_0}{2}} \sum_{k=1}^{N-1} \frac{\left[1 - p + \frac{p}{\eta}\cos(\theta_k)\right]^t U_{N-n_>-1}(\sigma) \left\{ f^{\frac{1}{2}} U_{n_<-1}(\sigma) - U_{n_<-2}(\sigma) \right\}}{-\lim_{\sigma \to \cos(\theta_k)} \frac{1}{\sin^2(\theta_k)} \left\{ N\left[f^{\frac{1}{2}} T_N(\sigma) - T_{N-1}(\sigma) \right] + T_{N-1} - \cos(\theta_k)\left[f^{\frac{1}{2}} U_{N-1}(\sigma) - U_{N-2}(\sigma) \right] \right\}}, \tag{B3}$$

and with some further algebraic manipulation we obtain Eq. (21) with $\gamma = m$.

APPENDIX C: CONTINUOUS TIME AND SPATIAL LIMITS OF THE ONE-DIMENSIONAL PROPAGATORS

The continuous space and time propagators of the biased lattice walk in finite domains, that is the drift-diffusion bounded propagator can be recovered by appropriate limiting procedures. We consider first the continuous-time discrete-space analog of the 1D propagators [i.e., Eq. (21) in the main text] given by $C_{n_0}^{(\gamma)}(n, \tau) = \sum_{s=0}^{\infty} W(s, \tau) P_{n_0}^{(\gamma)}(n, s)$ [46,47], where $W(s, \tau)$ is the probability of s jumps to occur in (continuous) time τ. With $\psi(\tau)$, the probability of a jump event to occur at time τ, one

can construct $\overline{W}(s, \epsilon) = \frac{1-\overline{\psi}(\epsilon)}{\epsilon}\overline{\psi}(\epsilon)$, where $\overline{f}(\epsilon) = \int_0^\infty e^{-\epsilon t} f(t)\mathrm{d}t$ is the Laplace transform of $f(t)$. Laplace transforming and evaluating the geometric sum yields

$$\overline{C}_{n_0}^{(\gamma)}(n, \epsilon) = \sum_{k=w^{(\gamma)}}^{W^{(\gamma)}} \frac{h_k^{(\gamma)}(n, n_0)[1 - \overline{\psi}(\epsilon)]}{\epsilon\left\{1 - \overline{\psi}(\epsilon)\left[1 + s_k^{(\gamma)}\right]\right\}}. \tag{C1}$$

Defining $\psi(\tau) = 2Re^{-2R\tau}$, where R is a rate, and its Laplace transform $\overline{\psi}(\epsilon) = 2R/(\epsilon + 2R)$, one can inverse Laplace transform Eq. (C1) obtaining the continuous-time discrete-space biased random walk in finite domains,

$$C_{n_0}^{(\gamma)}(n, \tau) = \sum_{k=w^{(\gamma)}}^{W^{(\gamma)}} h_k^{(\gamma)}(n, n_0)e^{2R\tau s_k^{(\gamma)}}. \tag{C2}$$

To take the continuous spatial limit of Eq. (C2), we consider a lattice spacing b with $b, g \to 0$ and $R, N, n, n_0 \to +\infty$, such that $x = bn$, $x_0 = bn_0$, $L = Nb$, $Rqb^2 \to D$, and $g/b \to v/2D$, where L is the domain size ($0 \leqslant x, x_0 \leqslant L$), D the diffusion constant and v the drift velocity. Evaluation of these limits requires different steps for each of the boundary conditions which are outlined in the following sections.

1. Absorbing boundaries

From Eq. (C2), the continuous-time discrete-space propagator with absorbing boundaries is given by

$$C_{n_0}^{(a)}(n, \tau) = \sum_{k=1}^{N-1} \frac{2f^{\frac{n-n_0}{2}} \sin\left[\left(\frac{n-1}{N-1}\right)k\pi\right] \sin\left[\left(\frac{n_0-1}{N-1}\right)k\pi\right]}{N-2} \exp\left\{-2Rq\tau\left[1 - \frac{1}{\eta}\cos\left(\frac{k\pi}{N-1}\right)\right]\right\}. \tag{C3}$$

The term $f^{\frac{n-n_0}{2}}$ in Eq. (C3) needs to be rewritten as $\exp\left[\frac{1}{2}(n-n_0)\ln(f)\right]$ before Taylor expansion of $\ln(f)$ with $f = \frac{1-g}{1+g}$ to obtain

$$\exp\left[\frac{1}{2}(n-n_0)\ln(f)\right] \to \exp\left[\frac{v(x_0-x)}{2D}\right], \tag{C4}$$

where $bn \to x$, $bn_0 \to x_0$ and $g/b \to v/(2D)$. The time-dependent term in Eq. (C2) requires a Taylor expansion of the $\cos(\theta)$ term around $\theta = 0$ and $\eta = (\sqrt{1-g^2})^{-1}$ around $g = 0$. With $Nb \to L$, one then has

$$2Rp\left[1 - \frac{1}{\eta}\cos\left(\frac{k\pi}{N-1}\right)\right] \to \frac{v^2}{4D} + \frac{D\pi^2 k^2}{L^2}. \tag{C5}$$

Combining these results we recover the continuous space-time solution to the drift-diffusion equation with absorbing boundaries (see e.g., Eq. (1.1.4-7) in Ref. [48]),

$$C_{x_0}^{(a)}(x, \tau) = \frac{2}{L}\sum_{k=1}^{\infty} \sin\left(\frac{k\pi x}{L}\right) \sin\left(\frac{k\pi x_0}{L}\right) \exp\left[-\frac{D\pi^2 k^2 \tau}{L^2} + \frac{2v(x_0-x) - \tau v^2}{4D}\right]. \tag{C6}$$

2. Reflecting boundaries

Using Eq. (C2), the continuous-time discrete-space propagator with two reflective boundaries is

$$C_{n_0}^{(r)}(n, \tau) = \frac{f^{n-1}(1-f)}{1-f^N} + \frac{2f^{\frac{n-n_0}{2}}}{N}\sum_{k=1}^{N-1} \frac{\left(f^{\frac{1}{2}}\sin\left[\frac{nk\pi}{N}\right] - \sin\left[(n-1)\frac{k\pi}{N}\right]\right)\left(f^{\frac{1}{2}}\sin\left[\frac{n_0 k\pi}{N}\right] - \sin\left[(n_0-1)\frac{k\pi}{N}\right]\right)}{1 + f - 2f^{\frac{1}{2}}\cos\left(\frac{k\pi}{N}\right)}$$

$$\times \exp\left\{-2Rp\tau\left[1 - \frac{1}{\eta}\cos\left(\frac{k\pi}{N}\right)\right]\right\}. \tag{C7}$$

For the continuous spatial limit the procedure is analogous to the case with two absorbing boundaries. The important differences with the absorbing case are the steady-state term,

$$\lim_{\tau \to \infty} C_{n_0}^{(r)}(n, \tau) = \frac{f^{n-1}(1-f)}{1-f^N}, \tag{C8}$$

and the $\frac{1}{2}(1+f) - f^{\frac{1}{2}}\cos\left(\frac{k\pi}{N}\right)$ term in Eq. (C7). Starting with the steady-state term and rewriting

$$\frac{f^{n-1}(1-f)}{1-f^N} = \frac{(1-f)\exp\left[(n-1)\ln(f)\right]}{1-\exp\left[N\ln(f)\right]}, \tag{C9}$$

one has to expand the $\ln(f)$ term, as done for the absorbing case, before taking the limits. The steady-state probability density in the continuous case becomes

$$\lim_{t \to \infty} C_{x_0}(x, \tau) = \frac{v \exp\left(\frac{vx}{D}\right)}{D\left[1 - \exp\left(\frac{vL}{D}\right)\right]}. \tag{C10}$$

For the terms inside the summation, it is convenient to expand the n and n_0 dependence first and rewrite

$$\frac{\left(f^{\frac{1}{2}} \sin\left[\frac{nk\pi}{N}\right] - \sin\left[(n-1)\frac{k\pi}{N}\right]\right)\left(f^{\frac{1}{2}} \sin\left[\frac{n_0 k\pi}{N}\right] - \sin\left[(n_0-1)\frac{k\pi}{N}\right]\right)}{1 + f - 2f^{\frac{1}{2}} \cos\left(\frac{k\pi}{N}\right)}$$

$$= \frac{\left\{\sin\left[\frac{nk\pi}{N}\right]\left(f^{\frac{1}{2}} \csc\left[\frac{k\pi}{N}\right] - \cot\left[\frac{k\pi}{N}\right]\right) + \cos\left[\frac{nk\pi}{N}\right]\right\}\left\{\sin\left[\frac{n_0 k\pi}{N}\right]\left(f^{\frac{1}{2}} \csc\left[\frac{k\pi}{N}\right] - \cot\left[\frac{k\pi}{N}\right]\right) + \cos\left[\frac{n_0 k\pi}{N}\right]\right\}}{(1+f) \csc^2\left[\frac{k\pi}{N}\right] + 2f^{\frac{1}{2}} \cot\left[\frac{k\pi}{N}\right] \csc\left[\frac{k\pi}{N}\right]}. \tag{C11}$$

With a Taylor expansion of $f^{\frac{1}{2}} \csc[\theta] - \cot[\theta]$, around $\theta = 0$, where $\theta = \frac{k\pi}{N}$ is the expansion variable, we find the limits

$$\lim_{\substack{N \to \infty \\ b, g \to 0}} \left\{ f^{\frac{1}{2}} \csc\left[\frac{k\pi}{N}\right] - \cot\left[\frac{k\pi}{N}\right] \right\} = -\frac{vL}{2Dk\pi}, \tag{C12}$$

similarly,

$$\lim_{\substack{N \to \infty \\ b, g \to 0}} \left\{ (1+f) \csc^2\left[\frac{k\pi}{N}\right] + 2f^{\frac{1}{2}} \cot\left[\frac{k\pi}{N}\right] \csc\left[\frac{k\pi}{N}\right] \right\} = \frac{v^2 L^2}{4D^2 k^2 \pi^2}. \tag{C13}$$

We finally recover the continuous space-time propagator with two reflective boundaries

$$C_{x_0}^{(r)}(x, \tau) = \frac{v \exp\left(\frac{vx}{D}\right)}{D\left[1 - \exp\left(\frac{vL}{D}\right)\right]} + \frac{2}{L} \exp\left[\frac{2v(x_0 - x) - \tau v^2}{4D}\right]$$

$$\times \sum_{k=1}^{\infty} \frac{\left\{\cos\left[\frac{k\pi x}{L}\right] - \mu_k \sin\left[\frac{k\pi x}{L}\right]\right\}\left\{\cos\left[\frac{k\pi x_0}{L}\right] - \mu_k \sin\left[\frac{k\pi x_0}{L}\right]\right\}}{\left(1 + \mu_k^2\right)} \exp\left(-\frac{D\pi^2 k^2 \tau}{L^2}\right), \tag{C14}$$

where $\mu_k = vL/(2Dk\pi)$, (e.g., see Eq. (1.1.4-8) in Ref. [48]).

3. Mixed boundaries

The discrete-space continuous-time propagator with mixed boundary conditions is

$$C_{n_0}^{(m)}(n, \tau) = \frac{2f^{\frac{n-n_0}{2}}}{N-1} \sum_{k=1}^{N-1} \frac{2f^{\frac{n-n_0}{2}} \sin[(N-n_>)\theta_k]\left\{f^{\frac{1}{2}} \sin[n_< \theta_k] - \sin[(n_< - 1)\theta_k]\right\}}{(N-1) \cos[(N-1)\theta_k] - N f^{\frac{1}{2}} \cos[N\theta_k]}$$

$$\times \exp\left\{-2Rq\tau\left[1 - \frac{1}{\eta} \cos\left(\frac{k\pi}{N-1}\right)\right]\right\}. \tag{C15}$$

Before taking the limits on the spatial dependence, it is necessary to study first the effect of the limits on the relationship

$$f^{\frac{1}{2}} U_{N-1}(\sigma) - U_{N-2}(\sigma) = 0. \tag{C16}$$

We rewrite the Chebyshev polynomials in Eq. (C16) using their trigonometric definition to yield

$$f^{\frac{1}{2}} \sin[N\mathrm{acos}(\sigma)] - \sin[(N-1)\mathrm{acos}(\sigma)] = 0. \tag{C17}$$

Expanding the $\sin[(N-1)\mathrm{acos}(\sigma)]$ results in the relationship

$$\tan[N\mathrm{acos}(\sigma)] = \frac{\sin[\mathrm{acos}(\sigma)]}{\cos[\mathrm{acos}(\sigma)] - f^{\frac{1}{2}}}. \tag{C18}$$

Defining $\theta_k = b\rho_k = \mathrm{acos}(\sigma)$ and substituting we find

$$\frac{\tan(L\rho_k)}{\rho_k \cos(b\rho_k)} = \frac{\sin(b\rho_k)}{\rho_k[\cos^2(b\rho_k) - f^{\frac{1}{2}} \cos(b\rho_k)]}, \tag{C19}$$

which, in the limit $b \to 0$ and $g \to 0$, results in the transcendental equation

$$\frac{\tan(L\rho_k)}{\rho_k} = \frac{2D}{v}. \tag{C20}$$

Expanding the numerator and denominator in the spatial dependence $h_k^{(m)}(n, n_0)$, and with the help of Eq. (C18) we find

$$h_k^{(m)}(n, n_0) = \frac{2f^{\frac{n-n_0}{2}}\left(\cos(\theta_k) - f^{\frac{1}{2}}\right)\{\tan(N\theta_k)\cos(n_<\theta_k) - \sin(n_>\theta_k)\}\{\tan(N\theta_k)\cos(n_<\theta_k) - \sin(n_<\theta_k)\}}{(N-1)[\cos(\theta_k) + \tan(N\theta_k)\sin(\theta_k)] - Nf^{\frac{1}{2}}}. \quad \text{(C21)}$$

With the $n_>$ dependence being equivalent to the $n_<$ dependence in Eq. (C21), we rewrite

$$h_k^{(m)}(n, n_0) = \frac{f^{\frac{n-n_0}{2}}}{B_k}[\tan(N\theta_k)\cos(n\theta_k) - \sin(n\theta_k)][\tan(N\theta_k)\cos(n_0\theta_k) - \sin(n_0\theta_k)], \quad \text{(C22)}$$

where

$$B_k = \frac{(N-1)[\cos(\theta_k) + \tan(N\theta_k)\sin(\theta_k)] - Nf^{\frac{1}{2}}}{2\left[\cos(\theta_k) - f^{\frac{1}{2}}\right]}.$$

After substituting $b\rho_k = \theta_k$, in the continuous limit we find

$$h_k^{(m)}(x, x_0) = \frac{1}{A_k}\exp\left[\frac{v(x_0 - x)}{2D}\right]\left[\tan(L\rho_k)\cos(x\rho_k) - \sin(x\rho_k)\right]\left[\tan(L\rho_k)\cos(x_0\rho_k) - \sin(x_0\rho_k)\right], \quad \text{(C23)}$$

where

$$A_k = \lim_{\substack{N \to \infty \\ b, g \to 0}} bB_k = \lim_{b, g \to 0}\left\{\frac{(L-b)[\cos(b\rho_k) + \tan(L\rho_k)\sin(b\rho_k)] - Lf^{\frac{1}{2}}}{2[\cos(b\rho_k) - f^{\frac{1}{2}}]}\right\} = -\frac{2D}{v} + \frac{L}{\cos^2(L\rho_k)}. \quad \text{(C24)}$$

Putting everything together we recover the continuous-time continuous-space solution (see Eq. (1.1.4-9) in Ref. [48]) with mixed boundary conditions,

$$C_{x_0}^{(m)}(x, \tau) = \exp\left[\frac{2v(x_0 - x) - \tau v^2}{4D}\right]\sum_{k=1}^{\infty}\frac{1}{A_k}\left[\tan(L\rho_k)\cos(x\rho_k) - \sin(x\rho_k)\right]\left[\tan(L\rho_k)\cos(x_0\rho_k) - \sin(x_0\rho_k)\right], \quad \text{(C25)}$$

where ρ_k are the roots of Eq. (C20).

4. Periodic boundaries

Starting with the discrete-space continuous-time propagator,

$$C_{n_0}^{(p)}(n, \tau) = \frac{1}{N}\sum_{k=0}^{N-1}\exp\left\{\frac{2k\pi i(n - n_0)}{N} - 2Rp\tau\left[1 - \cos\left(\frac{2k\pi}{N}\right) - ig\sin\left(\frac{2k\pi}{N}\right)\right]\right\}, \quad \text{(C26)}$$

one needs to expand the cos and sin terms before taking the limits resulting in the following continuous space-time propagator,

$$C_{x_0}^{(p)}(x, \tau) = \frac{1}{L}\sum_{k=0}^{\infty}\exp\left\{\frac{2k\pi i(x - x_0 + v)}{L} - \frac{4Dk^2\pi^2\tau}{L^2}\right\}, \quad \text{(C27)}$$

which clearly satisfies the periodic boundary condition. For higher dimensions, the limiting procedure can be carried through to give the continuous space-time analog which is the product of the one-dimensional propagators [Eqs. (C6), (C14), (C25), and (C27)] along each direction.

APPENDIX D: FIRST-PASSAGE PROBABILITY AND RELATED QUANTITIES WITH REFLECTING AND PERIODIC ONE-DIMENSIONAL DOMAIN

The first-passage probability, being the ratio of propagators in the z domain, can be constructed, respectively, for reflecting and periodic domains from Eqs. (16) and (C18), yielding

$$\widetilde{F}_{n_0}^{(r)}(n, z) = \frac{\widetilde{P}_{n_0}^{(r)}(n, z)}{\widetilde{P}_n^{(r)}(n, z)} = \begin{cases} \dfrac{f^{\frac{n-n_0}{2}}\left(f^{\frac{1}{2}}\sinh\left[n_0\operatorname{acosh}\left(\frac{\eta}{\beta}\right)\right] - \sinh\left[(n_0 - 1)\operatorname{acosh}\left(\frac{\eta}{\beta}\right)\right]\right)}{f^{\frac{1}{2}}\sinh\left[n\operatorname{acosh}\left(\frac{\eta}{\beta}\right)\right] - \sinh\left[(n-1)\operatorname{acosh}\left(\frac{\eta}{\beta}\right)\right]}, & n > n_0, \\[20pt] \dfrac{f^{\frac{n-n_0}{2}}\left(f^{\frac{1}{2}}\sinh\left[(N-n_0)\operatorname{acosh}\left(\frac{\eta}{\beta}\right)\right] - \sinh\left[(N+1-n_0)\operatorname{acosh}\left(\frac{\eta}{\beta}\right)\right]\right)}{f^{\frac{1}{2}}\sinh\left[(N-n)\operatorname{acosh}\left(\frac{\eta}{\beta}\right)\right] - \sinh\left[(N+1-n)\operatorname{acosh}\left(\frac{\eta}{\beta}\right)\right]}, & n < n_0, \end{cases} \quad \text{(D1)}$$

and

$$\widetilde{F}_{n_0}^{(p)}(n, z) = \frac{\widetilde{P}_{n_0}^{(p)}(n, z)}{\widetilde{P}_n^{(p)}(n, z)} = \begin{cases} \dfrac{f^{\frac{n-n_0}{2}}\left\{f^{\frac{1}{2}}\sinh\left[(N-n+n_0)\operatorname{acosh}\left(\frac{\eta}{\beta}\right)\right] + f^{-\frac{N}{2}}\sinh\left[(n-n_0)\operatorname{acosh}\left(\frac{\eta}{\beta}\right)\right]\right\}}{\sinh\left[N\operatorname{acosh}\left(\frac{\eta}{\beta}\right)\right]}, & n < n_0, \\[20pt] \dfrac{f^{\frac{n-n_0}{2}}\left\{f^{\frac{1}{2}}\sinh\left[(N-n_0+n)\operatorname{acosh}\left(\frac{\eta}{\beta}\right)\right] + f^{\frac{N}{2}}\sinh\left[(n_0-n)\operatorname{acosh}\left(\frac{\eta}{\beta}\right)\right]\right\}}{\sinh\left[N\operatorname{acosh}\left(\frac{\eta}{\beta}\right)\right]}, & n > n_0. \end{cases} \quad \text{(D2)}$$

Using Eqs. (D1) and (D2) yields the MFPT expressions in Eqs. (26) and (27) in the main text.

From the generating function of the return probability, $\widetilde{R}^{(r)}(n, z) = 1 - [\widetilde{P}_n(n, z)]^{-1}$, one can compute the MRT,

$$\mathcal{R}_n^{(r)} = \frac{1 - f^N}{f^{n-1}(1 - f)} \quad \text{and} \quad \mathcal{R}_n^{(p)} = N, \tag{D3}$$

which is, as expected from Kac's theorem, the reciprocal of the steady-state probability at the site.

First-passage probability when $g \pm 1$ and $q \neq 1$ with periodic boundary

Restricting the walker to move only forward or to remain at a site, that is no back-tracking, involves taking the limits $g \to \pm 1$, alternatively, $f \to 0$ or $f \to \infty$ in the first-passage probability expressions for the periodic domain. Although it is trivial to find the periodic propagator in Eq. (21) for such limits, the same cannot be said of the first-passage probability in Eq. (25) due to the term $f^{\frac{n-n_0}{2}}$. In the latter case it is much easier to derive the first-passage probability by separating the cases $n < n_0$ and $n > n_0$, and constructing the expression combinatorially. One can show that when $g = 1$ and $n < n_0$, or when $g = -1$ and $n > n_0$, the first-passage probability becomes

$$F_{n_0}^{(p)}(n, t) = \binom{t - 1}{t - |n - n_0|} q^{|n-n_0|}(1 - q)^{t-|n-n_0|}\Theta[t - |n - n_0|], \tag{D4}$$

while when $g = 1$ and $n > n_0$, or when $g = -1$ and $n < n_0$, it is

$$F_{n_0}^{(p)}(n, t) = \binom{t - 1}{t - (N - |n - n_0|)} q^{N-|n-n_0|}(1 - q)^{t-(N-|n-n_0|)}\Theta[t - (N - |n - n_0|)]. \tag{D5}$$

When Eq. (D4) applies, the probability of reaching the site is zero if the number of time steps is smaller than the displacement between the target and initial site, i.e., when $t < |n - n_0|$. At $t = |n - n_0|$, the relation $F_{n_0}^{(p)}(n, t) = q^{|n-n_0|}$ indicates that the walker may reach the target by always moving with each step giving a contribution equal to q to the probability. When $t > |n - n_0|$, the walker has a choice of remaining at any of the sites between n and n_0 (excluding n). In that case the coefficient $\binom{t-1}{t-|n-n_0|}$ represents all the possible combinations with which the walker can reach n from n_0 by making $|n - n_0|$ steps and $t - |n - n_0|$ pauses along the way. However, when Eq. (D5) applies, the walker travels around the domain with the length of the shortest possible path from n to n_0 being $N - |n - n_0|$, and the meaning of the terms are analogous to the case in Eq. (D4). The case $q = 1$ corresponds to a Kronecker δ in time: $F_{n_0}^{(p)}(n, t) = \delta_{t,|n-n_0|}$ or $F_{n_0}^{(p)}(n, t) = \delta_{t,N-|n-n_0|}$.

APPENDIX E: DERIVATION OF THE TWO-DIMENSIONAL PROPAGATOR

Solving the effective 1D Master equation Eq. (31), and taking the z transform gives

$$\widetilde{\widetilde{Q}}(n_1, \kappa_2, z) = \frac{\lambda_1 \left[e^{-i\kappa_2 n_{0_2}} f_2^{-\frac{n_{0_2}}{2}} \left(1 - f_2^{-1}\right) \right]}{1 - z\omega\left(1 - \frac{q_1}{2} + \frac{q_2}{2\eta_1} \cos[\kappa_2]\right)} + \frac{f_1^{\frac{n_1-n_{0_1}-1}{2}} e^{-i\kappa_2 n_{0_2}} f_2^{-\frac{n_{0_2}}{2}} \left(1 - f_2^{-1}\right)}{N_1} \sum_{k_1=1}^{N_1-1} \left\{ f_1^{\frac{1}{2}} \sin\left[\frac{n_1 k_1 \pi}{N_1}\right] - \sin\left[(n_1 - 1)\frac{k_1\pi}{N_1}\right] \right\}$$

$$\times \left\{ f_1^{\frac{1}{2}} \sin\left[\frac{n_{0_1} k_1\pi}{N_1}\right] - \sin\left[(n_{0_1} - 1)\frac{k_1\pi}{N_1}\right] \right\} \left\{ \eta_1 - \cos\left[\frac{k_1\pi}{N_1}\right] \right\}^{-1}$$

$$\times \left\{ 1 - z\left(1 - \frac{q_1}{2} - \frac{q_2}{2} + \frac{q_1}{2\eta_1} \cos\left[\frac{k_1\pi_1}{N_1}\right] + \frac{q_2}{2\eta_2} \cos[\kappa_2]\right) \right\}^{-1}, \tag{E1}$$

where

$$f_2 = \frac{1 - g_2}{1 + g_2}, \quad \eta_2 = \frac{1 + f_2}{2f_2^{\frac{1}{2}}} \quad \text{and} \quad \lambda_i = \frac{f_i^{n_i-1}(1 - f_i)}{1 - f_i^{N_i}}.$$

To find the analytic expression for the 2D random walker with bias and reflective boundaries in the first dimension, while diffusive and unbounded in the second dimension, one needs to inverse Fourier transform the second dimension to obtain

$$\widetilde{Q}(n_1, n_2 z)$$

$$= \lambda_1 \left\{ \frac{2\eta_2 f_2^{\frac{n_2-n_{0_2}}{2}} \varphi^{-|n_2-n_{0_2}|}}{z\omega q_2 \sinh\left[\text{acosh}\left(\frac{1}{\zeta}\right)\right]} \right\}$$

$$+ \frac{f_1^{\frac{n_1-n_{0_1}-1}{2}}}{N_1} \sum_{k_1=1}^{N_1-1} \frac{\left\{ f_1^{\frac{1}{2}} \sin\left[\frac{n_1 k_1\pi}{N_1}\right] - \sin\left[(n_1 - 1)\frac{k_1\pi}{N_1}\right] \right\} \left\{ f_1^{\frac{1}{2}} \sin\left[\frac{n_{0_1} k_1\pi}{N_1}\right] - \sin\left[(n_{0_1} - 1)\frac{k_1\pi}{N_1}\right] \right\}}{\eta_1 - \cos\left[\frac{k_1\pi}{N_1}\right]} \frac{2\eta_2 f_2^{\frac{n_2-n_{0_2}}{2}} \breve{\varphi}^{-|n_2-n_{0_2}|}}{z\omega q_2 \sinh\left[\text{acosh}\left(\frac{1}{\zeta}\right)\right]}, \tag{E2}$$

where (redefining)

$$\zeta = \frac{z\omega q_2}{2\eta_2\left[1 - z\omega\left(1 - \frac{q_2}{2}\right)\right]}, \quad \check{\zeta} = \frac{z\omega q_2}{2\eta_2\left\{1 - z\omega\left[1 - \frac{q_1}{2} - \frac{q_2}{2} + \frac{q_1}{2\eta_1}\cos\left(\frac{k\pi_1}{N_1}\right)\right]\right\}}, \quad \varphi = \exp\left[\mathrm{acosh}\left(\frac{1}{\zeta}\right)\right]$$

and

$$\check{\varphi} = \exp\left[\mathrm{acosh}\left(\frac{1}{\check{\zeta}}\right)\right].$$

On Eq. (E2), we use the method of images to impose the boundary condition following the procedure outlined in Appendix A 2 and asymmetrize the second dimension to yield

$$\widetilde{P}_{\vec{n}_0}^{(r_1, r_2)}(n_1, n_2 z) = \frac{2\lambda_1 \eta_2 f_2^{\frac{n_2 - n_{0_2}}{2}}}{zq_2 \sinh\left[\mathrm{acosh}\left(\frac{\eta_2}{\beta}\right)\right]} \left\{ \frac{\alpha^{N_2 - |n_2 - n_{0_2}|} + \alpha^{-N_2 + |n_2 - n_{0_2}|} - \alpha^{N_2 - |n_2 + n_{0_2}|}\xi - \alpha^{-N_2 + |n_2 + n_{0_2}|}\xi^{-1}}{\sinh\left[N_2 \mathrm{acosh}\left(\frac{\eta_2}{\beta}\right)\right]} \right\}$$

$$+ \frac{f_1^{\frac{n_1 - n_{0_1} - 1}{2}}}{N_1} \sum_{k_1 = 1}^{N_1 - 1} \frac{\left\{f_1^{\frac{1}{2}}\sin\left[\frac{n_1 k_1 \pi}{N_1}\right] - \sin\left[(n_1 - 1)\frac{k_1 \pi}{N_1}\right]\right\}\left\{f_1^{\frac{1}{2}}\sin\left[\frac{n_{0_1} k_1 \pi}{N_1}\right] - \sin\left[(n_{0_1} - 1)\frac{k_1 \pi}{N_1}\right]\right\}}{\eta_1 - \cos\left[\frac{k_1 \pi}{N_1}\right]}$$

$$\times \frac{2\eta_2 f_2^{\frac{n_2 - n_{0_2}}{2}}}{zq_2 \sinh\left[\mathrm{acosh}\left(\frac{\eta_2}{\check{\beta}}\right)\right]} \left\{ \frac{\check{\alpha}^{N_2 - |n_2 - n_{0_2}|} + \check{\alpha}^{-N_2 + |n_2 - n_{0_2}|} - \check{\alpha}^{N_2 - |n_2 + n_{0_2}|}\check{\xi} - \check{\alpha}^{-N_2 + |n_2 + n_{0_2}|}\check{\xi}^{-1}}{\sinh\left[N_2 \mathrm{acosh}\left(\frac{\eta_2}{\check{\beta}}\right)\right]} \right\}, \quad \text{(E3)}$$

where (redefining)

$$\beta = \frac{zq_2}{2\left[1 - z\left(1 - \frac{q_2}{2}\right)\right]}, \quad \check{\beta} = \frac{zq_2}{2\left\{1 - z\left[1 - \frac{q_1}{2} - \frac{q_2}{2} + \frac{q_1}{2\eta_1}\cos\left(\frac{k\pi_1}{N_1}\right)\right]\right\}}, \quad \alpha = \exp\left[\mathrm{acosh}\left(\frac{\eta_2}{\beta}\right)\right],$$

$$\check{\alpha} = \exp\left[\mathrm{acosh}\left(\frac{\eta_2}{\check{\beta}}\right)\right] \quad \xi = \frac{f_2^{\frac{1}{2}} - \alpha}{f_2^{\frac{1}{2}} - \frac{1}{\alpha}}, \quad \text{and} \quad \check{\xi} = \frac{f_2^{\frac{1}{2}} - \check{\alpha}}{f_2^{\frac{1}{2}} - \frac{1}{\check{\alpha}}}.$$

Employing the general identity Eq. (G1) (below) before inverse z transforming results in the time-dependent 2D propagator Eq. (32) found in the main text.

APPENDIX F: CONSTRUCTING PROPAGATORS OF HIGHER DIMENSIONS

To build a d-dimensional confined lattice random walk with bias, one first considers a semiconfined LRW where the first $d - 1$ dimensions are bounded while the final dth dimension is unbounded. Symmetrizing the dynamics in the dth dimension, yields a biased confined LRW in the $d - 1$ dimension while being diffusive and unconfined in the dth dimension. By Fourier transforming along the dth dimension reduces the problem to an effective $d - 1$-dimensional biased LRW whose solution is known. Solving for the dynamics in the (diffusive) dth dimension in the Fourier-z-domain and imposing boundary condition via the method of images, gives the solution to a confined random walk with bias in $d - 1$ dimensions and no bias in the dth dimension. Inverting the symmetrization procedure along the dth dimension yields the confined BLRW in d-dimensions in z-domain. Finally, with the use of the identities Eqs. (G1), (G2), Eq. (G4) or (G3) one inverts the propagator from the z-domain to the time domain. With such a procedure one can build propagators with arbitrary dimensions and arbitrary boundary conditions.

APPENDIX G: IDENTITIES OF FINITE TRIGONOMETRIC SERIES

For the derivation of the higher-dimensional propagators analytic identities can be obtained by equating the z-transform of Eq. (21) for each of the different boundary cases with the corresponding Eqs. (15), (16), and (18). For the reflecting condition we find

$$\frac{\left\{f^{\frac{1}{2}}U_{M-1-m_>}\left[\frac{\eta}{\gamma}(\gamma - \mu)\right] - U_{M-m_>}\left[\frac{\eta}{\gamma}(\gamma - \mu)\right]\right\}\left\{f^{\frac{1}{2}}U_{m_< - 1}\left[\frac{\eta}{\gamma}(\gamma - \mu)\right] - U_{m_< - 2}\left[\frac{\eta}{\gamma}(\gamma - \mu)\right]\right\}}{\mu U_{M-1}\left[\frac{\eta}{\gamma}(\gamma - \mu)\right]}$$

$$\equiv \frac{f^{\frac{m_1 + m_2 - 1}{2}}(f - 1)}{\mu(1 - f^M)} + \frac{1}{M}\sum_{k=1}^{M-1} \frac{\left\{f^{\frac{1}{2}}\sin\left[\frac{m_1 k\pi}{N}\right] - \sin\left[(m_1 - 1)\frac{k\pi}{M}\right]\right\}\left\{f^{\frac{1}{2}}\sin\left[\frac{m_2 k\pi}{N}\right] - \sin\left[(m_2 - 1)\frac{k\pi}{M}\right]\right\}}{\left(\eta - \cos\left[\frac{k\pi}{N}\right]\right)\left[\gamma - \mu - \frac{\gamma}{\eta}\cos\left[\frac{k\pi}{M}\right]\right]}, \quad \text{(G1)}$$

for the absorbing case we generate

$$\frac{U_{M-1-m_>}\left(\frac{\eta}{\gamma}\right)U_{m_<-2}\left(\frac{\eta}{\gamma}\right)}{U_{M-2}\left(\frac{\eta}{\gamma}\right)} \equiv \frac{1}{M-1}\sum_{k=1}^{M-1}\frac{\sin\left[\left(\frac{m_1-1}{M-1}\right)k\pi\right]\sin\left[\left(\frac{m_2-1}{M-1}\right)k\pi\right]}{\frac{\eta}{\gamma}-\cos\left[\frac{k\pi}{M-1}\right]}, \tag{G2}$$

and for the periodic domain we obtain

$$\frac{f^{\frac{m}{2}}\left[U_{M-1-|m|}\left(\frac{\eta}{\gamma}\right)+U_{|m|-1}\left(\frac{\eta}{\gamma}\right)f^{-\frac{M\,\mathrm{sgn}(m)}{2}}\right]}{T_M\left(\frac{\eta}{\gamma}\right)-T_M(\eta)} \equiv \frac{1}{M}\sum_{k=0}^{M-1}\frac{\exp\left(\frac{2k\pi i m}{M}\right)}{\frac{\eta}{\gamma}-\cosh\left[\frac{2k\pi i}{M}-\frac{1}{2}\ln(f)\right]}. \tag{G3}$$

In Eqs. (G1), (G2), and (G3) the meaning of the symbols are as follows: γ and μ are complex constants; M, m and n are integers with $1 \leqslant m_1, m_2 \leqslant N$; $f > 0$; $m_> = \frac{1}{2}(m_1 + m_2 + |m_1 - m_2|)$ and $m_< = \frac{1}{2}(m_1 + m_2 - |m_1 - m_2|)$; and $\eta = \frac{1}{2}(1 + f)f^{-\frac{1}{2}}$. The validity of Eqs. (G1) and (G2) is based on the known general identity Eq. (E1) in Ref. [22], while Eq. (G3) is a new identity that reduces to Eq. (E3) in Ref. [22] when $f, \eta = 1$. There is also a relation (numerical identity) that can be obtained from the mixed scenario using the procedure in Appendix B given by

$$\frac{U_{M-1-m_>}\left(\frac{\eta}{\gamma}\right)\left[f^{\frac{1}{2}}U_{m_<-1}\left(\frac{\eta}{\gamma}\right)-U_{m_<-2}\left(\frac{\eta}{\gamma}\right)\right]}{\left[f^{\frac{1}{2}}U_{M-1}\left(\frac{\eta}{\gamma}\right)-U_{M-2}\left(\frac{\eta}{\gamma}\right)\right]} \equiv \sum_{k=1}^{M-1}\frac{\sin[(M-m_>)\theta_k]\left\{f^{\frac{1}{2}}\sin[m_<\theta_k]-\sin[(m_<-1)\theta_k]\right\}}{\left\{(M-1)\cos[(M-1)\theta_k]-Mf^{\frac{1}{2}}\cos[M\theta_k]\right\}\left[\frac{\eta}{\gamma}-\cos(\theta_k)\right]}, \tag{G4}$$

where $\cos(\theta_k)$ is the kth (numerical) root of the orthogonal polynomial $f^{\frac{1}{2}}U_{M-1}[\cos(\theta)]-U_{M-2}[\cos(\theta)]$.

APPENDIX H: MEAN FIRST-RETURN TIMES IN HIGHER DIMENSIONS

A hint of the nontrivial dependence of the return dynamics can be evinced by studying how different initial positions affect the MRT. We display for this purpose in Fig. 7 the reciprocal of the MRT in a 2D domain with reflecting boundaries with different starting locations, $\vec{n}$, as a function of the bias $\vec{g}$. Each panel from Figs. 7(a)–7(d) represents a different starting location which is progressively closer to the top-left corner. In the presence of a bias, the walker is pushed away from the starting site. For an initial location at the center of the domain it results in a weak dependence on the bias direction as shown in Fig. 7(a). A strong dependence when the starting location is off-center is instead shown in Figs. 7(b)–7(d). With the shift in the starting sites from Fig. 7(b) to 7(c) to 7(d), there is a shorter MRT the stronger the bias is directed toward that corner ($g_1 \langle 0, g_2 \rangle 0$) with instead long MRT for all other bias directions. In Fig. 7(b), one may also notice an asymmetry with respect to the diagonal which is not present

in Figs. 7(c) and 7(d). It is due to the starting site being closer to the top boundary at $n_2 = N_2$ than the left boundary at $n_1 = 1$.

All panels in Fig. 7 display dependence on the bias strength. When the starting location is near the center, the bias toward a corner yields long MRTs when compared with a diffusive walker ($g_1 = g_2 = 0$) which has a natural tendency to stay near the starting location. Conversely, with the starting location at a corner, Fig. 7(d), one finds the shortest MRT when the walker is kept at the starting location with the bias $\vec{g} = (1, -1)$. Interestingly, when the starting location is off-centre and not at the boundary corner [Figs. 7(b) and 7(d)] the MRT is minimized for an intermediate bias strength. The latter is strong enough to reduce the number of trajectories traveling right or downwards from the starting site whilst weak enough to allow the walker to travel against the bias when near the top-left corner. The precise location of the minimum can be computed numerically for arbitrary dimensions from the explicit definition $\mathcal{R}_{\vec{n}}^{(\vec{r})} = \left[\prod_{j=1}^{(d)} h_{0_j}^{(\vec{r})}(n_j, n_j)\right]^{-1}$.
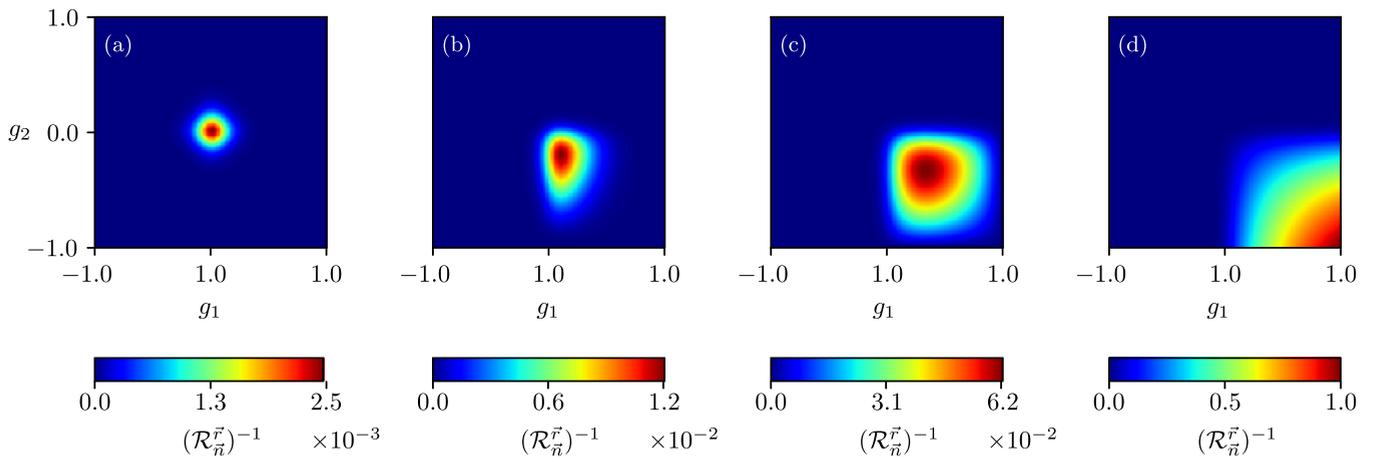
FIG. 7. The reciprocal of the MRT, $\left(\mathcal{R}_{\vec{n}}^{(\vec{r})}\right)^{-1}$, of a 2D BLRW with domain size $\vec{N} = (20, 20)$ and diffusion parameter $\vec{q} = (0.8, 0.8)$ as a function of the bias $\vec{g}$. Each panel from (a) to (d) represents different starting sites, respectively, $\vec{n} = (10, 10), (5, 18), (2, 19)$, and $(1, 20)$. A positive (negative) g_1 indicates a drift to the left (right), while a positive (negative) g_2 indicates a drift downwards (upwards).

[1] R. L. Schilling and L. Partzsch, *Brownian Motion: An Introduction to Stochastic Processes*, 1st ed. (De Gruyter Graduate, Berlin/Boston, 2012).

[2] B. D. Hughes, *Random Walks and Random Environments* (Clarendon Press/Oxford University Press, Oxford, UK, 1995).

[3] M. E. Fisher, Shape of a self-avoiding walk or polymer chain, J. Chem. Phys. **44**, 616 (1966).

[4] C. Godréche, S. N. Majumdar, and G. Schehr, Record statistics of a strongly correlated time series: Random walks and Lévy flights, J. Phys. A: Math. Theore. **50**, 333001 (2017).

[5] W. J. Ewens, *Mathematical Population Genetics: I. Theoretical Introduction* (Springer, New York, 2004).

[6] A. Okubo and S. A. Levin, *Diffusion and Ecological Problems: Modern Perspectives*, 2nd ed. (Springer Verlag, New York, NY, 2001).

[7] I. Lohmar and J. Krug, Diffusion-limited reactions and mortal random walkers in confined geometries, J. Stat. Phys. **134**, 307 (2009).

[8] G. Zumofen and A. Blumen, Energy transfer as a random walk. II. Two-dimensional regular lattices, J. Chem. Phys. **76**, 3713 (1982).

[9] R. M. Pearlstein, Exciton migration and trapping in photosynthesis, Photochem. Photobiol. **35**, 835 (1982).

[10] M. L. Mayo, E. J. Perkins, and P. Ghosh, First-passage time analysis of a one-dimensional diffusion-reaction model: Application to protein transport along DNA, BMC Bioinform. **12**, S18 (2011).

[11] J. Shin and A. B. Kolomeisky, Target search on DNA by interacting molecules: First-passage approach, J. Chem. Phys. **151**, 125101 (2019).

[12] B. F. Maier and D. Brockmann, Cover time for random walks on arbitrary complex networks, Phys. Rev. E **96**, 042307 (2017).

[13] P. Grassberger, How fast does a random walk cover a torus? Phys. Rev. E **96**, 012115 (2017).

[14] A. P. Riascos, D. Boyer, P. Herringer, and J. L. Mateos, Random walks on networks with stochastic resetting, Phys. Rev. E **101**, 062147 (2020).

[15] F. Thiel and I. M. Sokolov, Effective-medium approximation for lattice random walks with long-range jumps, Phys. Rev. E **94**, 012135 (2016).

[16] S. Redner, *A Guide to First-Passage Processes* (Cambridge University Press, Cambridge, UK, 2001).

[17] R. Metzler, G. Oshanin, and S. Redner, *First-Passage Phenomena and Their Applications* (World Scientific, Singapore, 2014).

[18] O. Bénichou and R. Voituriez, From first-passage times of random walks in confinement to geometry-controlled kinetics, Phys. Rep. **539**, 225 (2014).

[19] M. Kac, On the notion of recurrence in discrete stochastic processes, Bull. Amer. Math. Soc. **53**, 1002 (1947).

[20] S. Condamin, O. Bénichou, and M. Moreau, First-Passage Times for Random Walks in Bounded Domains, Phys. Rev. Lett. **95**, 260601 (2005).

[21] S. Condamin, V. Tejedor, and O. Bénichou, Occupation times of random walks in confined geometries: From random trap model to diffusion-limited reactions, Phys. Rev. E **76**, 050102(R) (2007).

[22] L. Giuggioli, Exact Spatiotemporal Dynamics of Confined Lattice Random Walks in Arbitrary Dimensions: A Century After Smoluchowski and Pólya, Phys. Rev. X **10**, 021045 (2020).

[23] B. D. Hughes, *Random Walks and Random Environments: Random Walks 1* (Clarendon Press, Oxford, UK, 1995).

[24] B. D. Hughes, *Random Walks and Random Environments: Random Walks 2* (Clarendon Press, Oxford, UK, 1995).

[25] V. Sourjik and N. S. Wingreen, Responding to chemical gradients: Bacterial chemotaxis, Curr. Opin. Cell Biol. **24**, 262 (2012).

[26] H. C. Berg, *Random Walks in Biology* (Princeton University Press, Princeton, NJ, 1993).

[27] G. Jékely, Evolution of phototaxis, Philos. Trans. Roy. Soc. B: Biol. Sci. **364**, 2795 (2009).

[28] O. Swei, J. Gregory, and R. Kirchain, Does pavement degradation follow a random walk with drift? Evidence from variance ratio tests for pavement roughness, J. Infrast. Syst. **24**, 04018027 (2018).

[29] N. A. Hill and D. P. Häder, A biased random walk model for the trajectories of swimming micro-organisms, J. Theor. Biol. **186**, 503 (1997).

[30] I. Mabrouki, G. Froc, and X. Lagrange, Biased random walk model to estimate routing performance in sensor networks, in *9ème Rencontres Francophones sur les Aspects Algorithmiques des Télécommunications* (Ile d'Oléron, France, 2007), p. 73.

[31] A. Valov, V. Avetisov, S. Nechaev, and G. Oshanin, Field-driven tracer diffusion through curved bottlenecks: Fine structure of first passage events, Phys. Chem. Chem. Phys. **22**, 18414 (2020).

[32] S. Godoy and S. Fujita, Reflection principles for biased correlated walks. Simple applications, J. Math. Phys. **33**, 2998 (1992).

[33] E. W. Montroll, Stochastic processes and chemical kinetics, in *Energetics in Metallurgic Phenomena: Vol III*, edited by W. Mueller (Gordon and Breach, New York, NY, 1967), pp. 122–187.

[34] L. Giuggioli, S. Gupta, and M. Chase, Comparison of two models of tethered motion, J. Phys. A: Math. Theor. **52**, 075001 (2019).

[35] M. Khantha and V. Balakrishnan, Hopping conductivity of a one-dimensional bond-percolation model in a constant field: Exact solution, Phys. Rev. B **29**, 4679 (1984).

[36] M. Khantha and V. Balakrishnan, Reflection principles for biased random walks and application to escape time distributions, J. Stat. Phys. **41**, 811 (1985).

[37] W.-C. Yueh, Eigenvalues of several tridiagonal matrices, Appl. Math. E-Notes **5**, 66 (2005).

[38] W.-C. Yueh and S. S. Cheng, Explicit eigenvalues and inverses of tridiagonal Toeplitz matrices with four perturbed corners, ANZIAM J. **49**, 361 (2008).

[39] A. R. Willms, Analytic results for the eigenvalues of certain tridiagonal matrices, SIAM J. Matrix Anal. Appl. **30**, 639 (2008).

[40] E. W. Montroll and G. H. Weiss, Random walks on lattices II, J. Math. Phys. **6**, 167 (1965).

[41] G. Pólya, Quelques problemes de probabilité se rapportant a la promenade au hasard? L'Enseignement Mathématique **20**, 8 (1919).

[42] G. Pólya, Über eine Aufgabe der Wahrscheinlichkeitsrechnung betreffend die Irrfahrt im Straßennetz, Math. Ann. **84**, 149 (1921).

[43] J. Abate, G. L. Choudhury, and W. Whitt, An introduction to numerical transform inversion and its application to probability

models, in *Computational Probability*, edited by W. Grassman (Kluwer, Boston, MA, 1999), pp. 257–323.

[44] W.-C. Yueh and S. S. Cheng, Explicit eigenvalues and inverses of several Toeplitz matrices, ANZIAM J. **48**, 73 (2006).

[45] G. F. A. D. L'Hôpital and J. Bernoulli, *L'Hôpital's Analyse Des Infiniments Petits: An Annotated Translation with Source Material by Johann Bernoulli*, No. 50 in Science Networks Historical Studies (Birkhäuser, Cham, 2015).

[46] E. W. Montroll and B. J. West, On an enriched collection of stochastic processes, in *Studies in Statistical Mechanics: Vol VII. Fluctuation Phenomena*, edited by E. Montroll and J. Lebowitz (North Holland Publishing, Amsterdam, 1979), pp. 61–175.

[47] P. Grigolini, The continuous time random walk versus the generalized master equation, Adv. Chem. Phys. **133**, 357 (2006).

[48] A. D. Polyanin, *Handbook of Linear Partial Differential Equations for Engineers and Scientists* (Chapman & Hall/CRC, Boca Raton, FL, 2002).